Accepted Manuscript

Quarterly Journal of Engineering Geology and Hydrogeology

A method to determine the relative importance of geological parameters that control the hydraulic erodibility of rock

Lamine Boumaiza, Ali Saeidi & Marco Quirion

DOI: https://doi.org/10.1144/qjegh2020-154

To access the most recent version of this article, please click the DOI URL in the line above. When citing this article please include the above DOI.

Received 18 September 2020
Revised 11 March 2021
Accepted 13 March 2021

Full title

A method to determine the relative importance of geological parameters that control the hydraulic erodibility of rock

Running header

Geological parameters controlling the rock erodibility

Authors name and affiliations

Lamine Boumaiza[1]*, Ali Saeidi[1], and Marco Quirion[2]

[1]Département des Sciences appliquées, Université du Québec à Chicoutimi, Chicoutimi (Québec), G7H 2B1, Canada

[2]Expertise en barrages, Direction Barrages et Infrastructures, Hydro-Québec, Montréal, (Québec), H2Z 1A4, Canada

*Corresponding author: E-mail address: lamine.Boumaiza@uqac.ca (L. Boumaiza)

Abstract

The most common methods used to evaluate the potential hydraulic erosion of rock are index-based methods, which correlate the force of flowing water and the capacity of a rock to resist erosion. This capacity is evaluated using erodibility indices, which combine a set of specific geological parameters. Nonetheless, there exists no clear consensus in regard to the relative importance assigned to the geological parameters. Our study proposes (i) a review of the existing index-based methods used to evaluate the hydraulic erodibility of rock, and (ii) a method to determine the relative importance of the geological parameters governing the erodibility of rock. The developed approach relies on a large data set of case studies providing details of unlined spillways subjected to erosion. We demonstrate that the analyzed geological parameters can be classified according to their relative importance—from highest to lowest—as follows: (1) joint shear strength, (2) nature of the potentially eroding surface, (3) rock block volume, (4) joint opening, (5) rock block's shape and orientation relative to flow direction, and (6) the rock mass deformation module. This ordering of the relative importance of the geological parameters agrees largely with previously established orderings that were based on field observations.

Keywords: Rock, Hydraulic erosion, Annandale's method, Pells's method, Kirsten's index, Erosion level.

Symbol notation list

D: Disturbance factor

E_{doa}: Erosion, discontinuity orientation adjustment

E_i: Young's modulus of intact rock (GPa)

eGSI: Erodibility geological strength index

E_{rm}: Rock mass deformation modulus (GPa)

GSI: Geological strength index

J_a: Joint surface alteration number

J_n: Joint set number

J_o: Joint opening (mm)

J_r: Joint roughness number

J_s: Relative block structure

K_b: Rock block size number

K_d: Joint shear strength number

LF: Likelihood factor

MR: Modulus ratio

M_s: Compressive strength number

N: Kirsten's index

NPES: Nature of the potentially eroding surface

P_a: Available hydraulic stream power (kW/m^2)

RF: Relative importance factor

RMR: Rock mass rating system

RMEI: Rock mass erosion index

RQD: Rock quality designation

S: Slope (°)

UCS: Unconfined compressive strength (MPa)

V_b: Rock block volume (m^3)

σ_{ci}: Uniaxial compressive strength (MPa)

The most common methods used for evaluating the potential hydraulic erosion of rock are those based on the correlation between the force of flowing water and the capacity of rock to resist the erosive force, such as Annandale's method (Annandale 1995) and Pells's methods (Pells 2016). The erosive force of flowing water usually called the available hydraulic stream power (P_a), is the hydraulic energy (expressed in kW/m^2) generated by the flowing water (Henderson 1966). The resistance capacity of rock can be evaluated using selected geological parameters that, when put into an equation, form an index. Van Schalkwyk (1989), Pitsiou (1990), and Moore (1991) demonstrated that some engineering classification systems of rock used to evaluate the mechanical excavatability of rock include most of the parameters that affect the hydraulic erodibility[1] of rock. Van Schalkwyk et al. (1994a) tested several rock characterization indices, such as the rock mass rating (*RMR*) system (Bieniawski 1973), the Q-system (Barton *et al.* 1974), both developed for assessing underground excavation stability and designing tunnel support, and Kirsten's index (Kirsten 1982, 1988) developed to evaluate the excavatability of earth materials. They found that these indices generated similar results; however, Kirsten's

[1] For this paper, we consider the terms "erodibility", "scour", and "hydraulic erosion" as being synonymous technical terms that describe the significant localized erosion of rock when the rock is submitted to hydraulic erosive power.

index tended to be more accurate. Following this assessment, this index has been most often adopted for evaluating the hydraulic erodibility of earth materials (Dooge 1993; Annandale and Kirsten 1994; Moore *et al.* 1994; Van-Schalkwyk *et al.* 1994b, a; Annandale 1995; Kirsten *et al.* 1996). Kirsten's index (*N*) (Eq. 1) is determined based on a selection of geological parameters related to the rock, such as the unconfined compressive strength (*UCS* expressed in MPa) of rock (M_s), rock block size (K_b), joint shear strength (K_d), and relative block structure (J_s).

$$N = M_s \cdot K_b \cdot K_d \cdot J_s \quad (1)$$

Kirsten (1982) adopted the Jennings et al. (1973) *UCS* classification to propose a descriptive chart that has M_s ratings ranging from 0.87 to 280. The K_b factor was initially introduced by Cecil (1970), who combined the rock quality designation index (*RQD*) with the joint set number (J_n). This factor, corresponding to RQD/J_n, was later adopted by Kirsten (1982) for his *N* index. As *RQD* can vary from 5%-100% (Barton *et al.* 1974), and J_n values can vary from 1-5 (Kirsten 1982, 1988), the K_b rating consequently ranges from 1-100. The K_d factor, representing joint shear strength is expressed as the ratio J_r/J_a where J_r is the rating corresponding to joint roughness, and J_a is the rating corresponding to joint surface

alteration. The J_r rating for joint conditions ranges from 0.5-4, whereas the J_a rating varies from 0.75-18 (Kirsten 1982). Accordingly, the K_d rating varies from 0.03-5.33. The J_s factor represents the effect of rock block's shape and orientation relative to the direction of flow. Its rating, as proposed by Kirsten (1982) for the orthogonal fractured systems, ranges from 0.37-1.5; its rating is from 0.09 to 1.38 for non-orthogonal fractured systems (Boumaiza *et al.* 2019b).

Recently, Pells (2016) proposed two other indices to assess the capacity of a rock to resist flowing water. The first, *eGSI* (Erodibility geological strength index) represents a modification of *GSI* (geological strength index), an index developed by Hoek et al. (1995) to characterize the rock environments. When the *GSI* index is determined using the *RMR* system, the discontinuity orientation factor is removed from *RMR* (Bieniawski 1976). Pells (2016) proposed the *eGSI* index by including a new discontinuity orientation adjustment factor (E_{doa}) to represent the effect of a rock block's shape and orientation relative to the direction of flow (Eq. 2).

$$eGSI = GSI + E_{doa} \tag{2}$$

The second index proposed by Pells (2016) is the rock mass erosion index (*RMEI*). It can be determined based on the relative importance factor (*RF*) and likelihood factor (*LF*) as presented in Eq. 3. The prefixes *P1* to *P5* in Eq. 3 are various sets of parameters (introduced in classification system) that represent, respectively, the kinematically viable mechanism for detachment, the nature of the potentially eroding surface, the nature of the joints, the joint spacing, and the rock block shape (Pells 2016).

$$RMEI = (RF_{P1}.LF_{P1}).(RF_{P2}.LF_{P2}).[(RF_{P3}.LF_{P3}) + (RF_{P4}.LF_{P4}) + (RF_{P5}.LF_{P5})] \quad (3)$$

Pells (2016) assumed that the existing indices, including Kirsten's index, did not represent the erosion mechanism observed in the field. Accordingly, the *RMEI* system attempts to represent the geological parameters controlling the erosion mechanism, where their relative importance is assumed based on the field observations of eroded rocky spillways. The most important geological parameters are weighted by a high *RF* value compared with those judged as less important. The kinematically viable mechanism for detachment and the nature of the potentially eroding surface are both weighted with a high *RF* value of 3, compared to the nature of the joints (*RF* = 2), joint spacing (*RF* = 1), and rock block shape (*RF* = 1). The structure of the *RMEI* system for hydraulic erosion could be considered as being similar to the Q-system (Barton *et al.* 1974)

that was also developed from field investigations. In the *RMEI* system (Pells 2016), rock block size is not included directly; however, joint spacing can provide an idea of rock block size given that a greater spacing of joints begets a greater rock block volume. Joint shear strength is also not included in the *RMEI* classification, but the nature of the joint can be considered as its synonym factor given that this factor incorporates the natural condition of joints. The *RMEI* classification considers the joint spacing factor to be less important (*RF* = 1) than the nature of the joints, which is weighted as *RF* = 2. The Q-system, on the other hand, places more importance on the K_b factor (rating range from 1 to 100; indicating the rock block size) than the K_d factor (rating range from 0.03 to 5.33; representing joint shear strength) (Barton *et al.* 1974). The discordance of the relative importance of the parameters included in these two classification systems demonstrates that the evaluation in the field can be influenced greatly by the judgment of the analyst. The subjective judgment of geological parameters included within Pells's methods (Pells 2016) and the other Kirsten's index–based methods (Moore et al. 1994; Van-Schalkwyk et al. 1994a,b; Annandale 1995; Kirsten et al. 1996) can greatly affect the weight attributed to each geological parameter and, subsequently, influence the assessed index value used for evaluating the hydraulic erodibility of rock. Pells (2016), who investigated numerous rocky unlined spillways, underlined the degree of scatter related to subjectivity in the interpretation of rock indices. Results from a large geological characterization and mapping campaign, conducted by a group of independent engineers, confirmed a significant variability for the interpreted observations; this variability reflected as range of assessed values of geological parameters (Pells 2016).

As rock scour is a highly complicated process (Bollaert and Schleiss, 2003), any assessment should begin by determining the relevant geological parameters applicable to its evaluation. This initial selection should then be coupled with determining the relative

importance of the selected geological parameters. The main objective of this paper is to develop a method that determines the relative importance, via classification, of the geological parameters that control hydraulic erosion. Our method emerges from observing the errors produced when evaluating the hydraulic rock scour using existing methods.

1 Analysis of comparative methods

At present, dam spillway design relies largely on a "scour threshold" methods to assess the hydraulic rock erosion; these methods exist as a function of P_a and an erodibility index (Mörén and Sjöberg 2007; Hahn and Drain 2010; Pells *et al.* 2015). The "scour threshold" used within a suite of methods is determined from the interpreted erosion observed for various case studies. The threshold emerges from plotted data and a threshold line that separates case studies having observable specific scour conditions from those lacking significant scour.

1.1 Background of comparative methods based on Kirsten's index

Van Schalkwyk et al. (1994a) categorized the erosion conditions of certain classes as a function of erosion depth (Table 1). This classification was updated (Table 2) (Van Schalkwyk et al., 1994b) by adding the data of Moore et al. (1994). This update to the erosion classification subsequently altered the level of scour threshold lines.

Annandale (1995) used Kirsten's index to analyze the collected data of Moore et al. (1994), and Van Schalkwyk et al. (1994a). By plotting this data in relation to P_a, Annandale (1995) proposed a single scour threshold line that separated scour and no-scour events. He considered scour conditions when the erosion depth exceeded 2 m, as less than 2 m of erosion is considered relatively inconsequential, as it is most often the result of loose blocks of rock being removed from the stratum surface (Annandale 2006). Applying the same concept as Annandale (1995), Kirsten et al. (2000) incorporated data from Dooge (1993) and Moore et al. (1994) to propose an alternative scour threshold line separating scour and no-scour conditions.

Given that the scour threshold lines proposed by Annandale (1995) and Kirsten et al. (2000) are based on the same evaluation of erosion conditions (>2 m = scour, <2 m = no scour), these threshold lines can be plotted together. The concept proposed by Van Schalkwyk et al. (1994a) cannot be compared as it does not consider an erosion limit depth of 2 m (Table 1). However, the proposal of Van Schalkwyk et al. (1994b) can be compared to that of Annandale (1995) and Kirsten et al. (2000) by considering together the "negligible", "minor", and "moderate" classes (Table 2) as being no-scour (<2 m), and the "large" class as representing scour conditions (>2 m). The lines that demarcate the interpreted onset of scour based on Kirsten's index versus P_a are summarized in Figure 1.

1.2 Background to the Pells's methods

Adopting the same concept of Van Schalkwyk et al. (1994b), Pells (2016) categorized the erosion conditions for certain classes by slightly modifying the depth of the eroded area. He also added information related to the extent of the eroded

area (Table 3). Using the *eGSI* index (Eq. 2) and *RMEI* index (Eq. 3), Pells (2016) plotted their calculated values versus P_a to manually determine the selected erosion classes. These classes are separated by scour threshold lines, as shown in Figures 2 and 3. Figure 3, as proposed originally by Pells (2016), was recently modified by Douglas et al. (2018). However, it is not clear whether an optimizing process was used to determine the placement of the updated threshold lines.

2 Comparative analysis

Our comparative analysis includes: 1) comparing all comparative scour threshold methods (the Van Schalkwyk, Annandale, Kirsten, and Pells methods); 2) comparing the Van Schalkwyk and Pells methods; and 3) comparing the two Pells's methods separately. For this comparative analysis, we use field data collected from the case studies, collected by Pells (2016), from unlined rocky spillways of selected dams in Australia and South Africa. 86 case studies provide a complete dataset for all values of the three erodibility indices (Kirsten's index, the *eGSI* index, and the *RMEI* index) being compared. The principle for representing a case study consists of plotting the value of the erodibility index (Kirsten's index *N*, *eGSI*, or *RMEI*) along the x-axis of the chart with the value of the hydraulic stream power (P_a) along the y-axis. Information related to the erodibility indices and the hydraulic stream power of the case studies is presented in Appendix 1.

2.1 Comparing all methods

To compare the existing methods, we harmonized the different erosion classes as the Annandale and Kirsten methods are based on two scour classes, whereas the Van Schalkwyk and Pells methods are based on several scour classes. By assuming that scour conditions exist when erosion depth is >2 m (Annandale 2006), Pells's charts (Figures 2 and 3) could be interpreted as a single scour threshold. Indeed, the erosion condition classes of "negligible", "minor", and "moderate" (Table 3) can be grouped to represent the "no-scour" condition as the erosion depth of these classes is <2 m. The "large" and "extensive" classes (Table 3) can represent the "scour" condition as their erosion depth is >2 m. Accordingly, the considered scour threshold line is that separating the "moderate" and "large" classes. As introduced in Section 2.1, the Van Schalkwyk, Annandale and Kirsten scour thresholds can be presented together (Figure 1) given that scour is assumed to occur when erosion is >2 m. The 86 case studies plotted according to Kirsten's index, the *eGSI* index and the *RMEI* index are presented in Figures 4a, 4b, and 4c, respectively.

We can determine the efficacy of these developed scour thresholds by the number of case studies having a poorly evaluated scour condition. Annandale and Van Schalkwyk methods differ marginally from Kirsten's threshold (Table 4). Annandale's method (Annandale 1995, 2006), however, is the most commonly used method for evaluating hydraulic rock scour (Mörén and Sjöberg 2007; Hahn and Drain 2010; Laugier *et al.* 2015; Rock 2015; Castillo and Carrillo 2016). We observe an improvement when we include the erodibility indices of *RMEI* and *eGSI*. These recently developed indices were developed specifically for evaluating the hydraulic erodibility of rock; Kirsten's index, in contrast, was initially proposed for evaluating the mechanical excavatability of earth materials.

2.2 Comparing the Van Schalkwyk and Pells methods

As both of the proposed Van Schalkwyk's classifications (Tables 1 and 2) and that of Pells (Table 3) categorize the erosion condition within a number of classes, comparing these methods will assess their respective efficacies when different erodibility indices (Kirsten's index, *eGSI* index, and *RMEI* index) are applied. Comparison, therefore, included a greater number of erosion classes than when we compared the pair of classes in Section 3.1. As the three erosion classifications

(presented in Tables 1, 2, and 3) differ, we optimally harmonize the classification systems using Table 2 (Van Schalkwyk et al., 1994b; an update to Table 1) and Table 3 (Pells 2016). The final harmonized classification includes the classes "negligible" (<0.2 or 0.3 m depth), "minor to moderate" (0.2 to 2 m depth), and "large to extensive" (>2 m depth). The plotted data based on the Van Schalkwyk, *eGSI*, and *RMEI* methods are shown in Figures 5a, 5b, and 5c, respectively.

The Van Schalkwyk et al. (1994b) method produces a high committed error percentage (77%) for the "large to extensive" class (Table 5), while the committed error percentage was highest for the "minor to moderate" using the Pells's methods (29%). The discordance between the Van Schalkwyk et al. (1994b) and Pells's methods is also observed for the least committed error; the "negligible" class has the least committed error (14%) according to the Van Schalkwyk et al. (1994b) method, while the "large to extensive" class has values of 15% and 8% for the *eGSI* and *RMEI* methods, respectively. Furthermore, the "negligible" erosion condition class of Van Schalkwyk et al. (1994b) provides less committed error than those of Pells. However, the Pells's methods provide less committed error for the "minor to moderate" and "large to extensive" erosion condition classes. For two erosion

classes ("minor to moderate" and "large to extensive"), the recently developed method of Pells provides a better evaluation than that of Van Schalkwyk et al. (1994b), the latter based on Kirsten's index. This pattern could be related to the recent indices of Pells (2016) that are especially proposed for evaluating the hydraulic erodibility of rock.

2.3 Comparing the Pells methods

2.3.1 Comparisons based on erosion classes

As the Pells's methods (*RMEI* and *eGSI*) categorize erosion condition with the same classes (Table 3), we can compare the committed error of each method and verify the ranking of the eventual committed error. The error is determined here using the number of case studies where the scour condition is poorly evaluated. The plotted case studies, based on the *eGSI* and *RMEI* indices, are shown in Figures 6a and 6b, respectively.

From the plotted *eGSI* index dataset (Figure 6a), 42 case studies are evaluated poorly, corresponding to a committed error of 49% from all considered case studies. The plotted *RMEI* index dataset has 35 poorly evaluated case studies (Figure 6b),

corresponding to a committed error of 41%. Overall, the *RMEI* method provides a better evaluation of the two indices. Nonetheless, the rank of the committed error is very high for both approaches (41% for *RMEI*; 49% for *eGSI*). Observing the individual erosion classes, the highest committed error is found in the "extensive" class of the *RMEI* method (63%) and in the "minor" class of the *eGSI* method (68%) (Table 6, Figure 7). Differences exist between *RMEI* and *eGSI* for the least committed error as the "negligible" class has the least committed error based on the *RMEI* method (30%), while the "large" class has the least committed error using *eGSI* (17%). The *RMEI* committed error percentage follows an upward trend, whereas *eGSI* committed error percentage follows an irregular trend between classes (Figure 7). Furthermore, the erosion condition classes of "negligible", "minor", and "moderate" using *RMEI* generate lower committed error percentages than the *eGSI* method. *RMEI*, however, has a higher committed error than *eGSI* for the "large" and "extensive" classes. Based on the observed discordance between the *RMEI* and *eGSI* methods, we can conclude that the *RMEI* and *eGSI* methods cannot be used simultaneously for assessing the planned spillway project.

2.3.2 Comparisons based on hydraulic stream power class

As the hydraulic rock scour mechanism is controlled by the rock resistance capacity and the erosive force of water, a comparative analysis is performed by taking into account the effect of the subsequent variations of P_a. The committed error is calculated for each P_a class by determining the number of case studies where scour condition is poorly evaluated within the considered P_a class. The P_a classes for this purpose (0-2.5, 2.5-5, 5-10, 10-25, 25-50, and >50 kW/m^2) are adopted by Boumaiza *et al.* (2019a). The calculated committed errors are illustrated in Figure 8.

In general, the *eGSI* method generates a higher committed error than the *RMEI* method (Figure 8). However, for four P_a classes (2.5-5, 5-10, 25-50, and >50 kW/m^2), the committed error difference between *RMEI* and *eGSI* varies around 10% or less. The significant difference in committed error is observed for the 10–15 and 15–25 kW/m^2 P_a classes, whereas the *RMEI* method produces less committed error than the *eGSI*. This difference is likely related to the effect of subjective judgment used for the case studies submitted to a P_a ranging between 10 and 25 kW/m^2. The behavior of the *RMEI* committed error curve generally matches that of the *eGSI* curve, and thus demonstrates a concordance between *RMEI* and *eGSI*. Moreover, the P_a classes of 2.5-5 and 5-10 present a high and low committed error, respectively, for both methods, and similar values for the >50 kW/m^2 class. Thus, hydraulic conditions

tend not to affect *RMEI* nor *eGSI*. If hydraulic conditions have less effect on the committed error, attention should focus more on the geological parameters. A focus on geological parameters can improve the methods used for evaluating the hydraulic rock scour, and attempts to improve these methods must include two main steps: 1) identify the relevant geological parameters for evaluating hydraulic rock scour, and 2) determine the relative importance of the selected geological parameters. Boumaiza *et al.* (2019a) analyzed a set of geological parameters related to hydraulic erosion and proposed a method for determining the relevant geological parameters. Boumaiza *et al.* (2019a) highlighted that hydraulic erodibility is governed by specific geological parameters. In the following section, we detail how to determine the relative importance of the determined geological parameters and present a developed method. We then compare the outcomes of this developed method with field observations.

3 Description of the method

The proposed method for determining the relative importance of the geological parameters that control the hydraulic erodibility of rock is summarized in Figure 9. Each methodological step is described in the following subsections.

3.1 Step 1 - Selecting a geological parameter

Using their developed method, Boumaiza *et al.* (2019a) examined a set of geological parameters to determine those considered to be relevant for evaluating the hydraulic erodibility of rock. Briefly, they collected compiled data from case studies conducted on unlined rocky dam spillways (Pells 2016); this data included all available information related to the set of parameters characterizing rock, the P_a, and the observed erosion (i.e., "negligible", "minor", "moderate", "large" and "extensive") that were labeled with an erosion level of 1, 2, 3, 4, and 5, respectively. Boumaiza *et al.* (2019a) assessed the selected parameters individually, each parameter classified according to an existing classification from the literature or a proposed statistical classification. As there were several case studies within the same class, they calculated the mean level of erosion for a given P_a category and then ran the identical calculation process for all P_a categories. Each series of calculations for the P_a categories were run for all classes of a single geological parameter. A best-fit curve for the calculated mean level of erosion versus the average P_a was then plotted. Boumaiza *et al.* (2019a) identified these best-fit curves as the sensitivity curves to erodibility that produce a synthetic value of the potential level of erosion at a given value of P_a. Only those parameters having sensitivity curves to erodibility that presented a logical sequence within the plot was considered to be relevant. The retained parameters were joint opening (J_o), joint

shear strength (K_d), rock block volume (V_b), the parameter representing the block's shape and orientation relative to the flow direction (E_{doa}), and the nature of the potential eroding surface (*NPES*).

By applying this approach of Boumaiza *et al.* (2019a), we can examine the rock mass deformation modulus (E_{rm}) as it is a representative parameter of a rock subjected to hydraulic loading. We calculate E_{rm} of the eroded case studies using Eq. 4 (Hoek and Diederichs 2006).

$$E_{rm} = E_i \left[0.02 + \frac{1-D/2}{1+e^{((60+15D-GSI)/11)}}\right] \quad (4)$$

where E_i is Young's modulus of intact rock (GPa), D is the disturbance factor, and *GSI* is the geological strength index. We use the *GSI* values available in Pells (2016) for the eroded case studies and assume the D factor to be 0.7 (Hoek *et al.* 2002). However, E_i was not reported for the eroded case studies. As both the rock type and uniaxial compressive strength of the eroded case studies are available in Pells (2016), we use Eq. 5 (Hoek and Diederichs 2006) to determine E_i:

$$E_i = MR.\ \sigma_{ci} \quad (5)$$

where *MR* is the modulus ratio that can be determined as a function of the rock type. Depending on the rock type of the eroded case studies, the *MR* is determined from the compiled available data of the *RocData* software (Rocsciences 2019). σ_{ci} is the uniaxial compression strength of intact rock. The available σ_{ci} values in Pells (2016) for the

erosion case studies are used in this study. Other alternatives for determining σ_{ci} according to the type of rock can be found in Mustafa *et al.* (2015, 2016). The *GSI*, rock type, *UCS* (expressed in MPa), *MR*, and the calculated E_i and E_{rm} are tabulated in Appendix 1. As there is no existing classification system for E_{rm}, we can build one by evaluating the case studies of eroded unlined rocky dam spillways (Table 7), taking inspiration from Fattahi et al. (2019).

As E_{rm} indicates the resistance of a rock mass to deformation, a rock mass of E_{rm} Class 1 (E_{rm} = 0-10 GPa), as described in Table 4, should be more sensitive to erodibility than other rock masses (e.g., an E_{rm} of Class 4 with E_{rm} is >30 GPa). Sensitivity curves to erodibility based on the E_{rm} classification (Table 7) are shown in Figure 10. The Class 3 sensitivity curve related to (20–30 GPa) shows a relatively lower correlation coefficient (R^2 = 0.2). Nonetheless, the general mean value of the R^2 related to all the curves is about 0.7, which can be considered as a representative value for all the obtained results.

The best-fit curves follow perfectly the E_{rm} categories (Figure 10). Class 4 (E_{rm} >30 GPa) case studies are least sensitive to erodibility, and sensitivity is greater as E_{rm} decreases. With a P_a value of 10 kW/m^2, for example, a Class 4 rock mass (E_{rm} >30 GPa) would have negligible to minor erosion, while a Class 1 rock mass (E_{rm}

= 0-10 GPa) would experience moderate erosion. As E_{rm} sensitivity curves to erodibility show a logical sequence having a proportional relationship between E_{rm} and the level of erosion (when E_{rm} decreases, erosion is greater), E_{rm} can be retained as a relevant parameter for evaluating the hydraulic erodibility of rock. E_{rm} can be added to the set of relevant parameters (J_o, K_d, V_b, E_{doa}, and *NPES*) retained previously by Boumaiza *et al.* (2019a) for evaluating the hydraulic erodibility of rock. We consider all of these relevant parameters to determine their relative importance in hydraulic erosion mechanism. Each parameter is assessed individually (Steps 1–5, Figure 9). The process is then repeated from Step 6 to the end for the considered geological parameters. To explain our method, we introduce the J_o parameter into the analysis process (Steps 1–6).

3.2 Step 2 - Selecting a hydraulic stream power

Boumaiza *et al.* (2019a) proposed J_o sensitivity curves to erodibility (Figure 11) based on Bieniawski's (1989) J_o classification (J_o classes are indicated in the legends of Figure 11). These sensitivity curves to erodibility (Figure 11) produce a synthetic value for the level of potential erosion at a given value of P_a. Sensitivity curves related to the <0.25 mm and 0.25–0.5 mm classes have a R^2 = 0.4. However, the general mean value of the R^2 related to all the curves is about 0.6, a value that can be considered as representative for all the obtained results. In Step 2, we select a given P_a value of 2 kW/m^2. This value can occur in actual study cases and is selected to determine erosion level, as explained in Step 3.

3.3 Steps 3 and 4 - Determining erosion level based on the selected P_a

Using Figure 11, the best-fit curve equation of each J_o class is used to determine the erosion level (*EI*), where the P_a value is kept at 2 kW/m^2. Step 3 determines the erosion level when different J_o classes are subjected to same P_a, and therefore provides an overview of erosion level behavior versus J_o. The same process is then repeated for the other P_a (Step 4). For this analysis, we select P_a values of 2, 10, and 40 kW/m^2 to represent a range of increasing P_a. The main objective of Step 4 is to determine the erosion level behavior for J_o classes when these classes are subjected to various P_a. The calculated erosion level for the subsequent J_o classes, based on the three selected P_a, are presented in Table 8 and Figure 12. It should be noted that the J_o classes <0.25 mm, 0.25–0.5 mm, 0.5–2.5 mm, and 2.5–10 mm (Table 8) are represented in Figure 12 as 0.25, 0.5, 2.5, and 10 mm, respectively.

The best-fit J_o hydraulic sensitivity curves to erodibility represent the calculated erosion level versus J_o classes as related to the P_a value (2, 10, and 40 kW/m^2). These best-fit curves (hereafter named hydraulic sensitivity curves to erodibility) illustrate a proportional relationship between J_o and erosion level. When J_o increases, the erosion level becomes greater, and this pattern is observed for all three selected P_a values.

3.4 Steps 5 and 6 - Determining the slope of the hydraulic sensitivity curves to erodibility for the selected geological parameters

We then calculate the slope of the hydraulic sensitivity curves to erodibility using the equation of the best-fit curve (Figure 12). The calculated slopes for J_o hydraulic sensitivity curves to erodibility are proportional to P_a (Figure 12). The hydraulic sensitivity curve having the steepest slope is P_a = 40 kW/m^2 (9°), followed by P_a = 10 kW/m^2 (8.05°), and P_a = 2 kW/m^2 (6.94°), respectively (Figure 12). The steepest hydraulic sensitivity curve includes the highest erosion levels and, consequently, corresponds to an important erosion effect compared with other lower-sloped hydraulic sensitivity curves. However, these slopes are controlled mostly by P_a.

Following the same process as that used for the J_o parameter, we analyze all the selected geological parameters using the sensitivity curves to erodibility (Appendix 2). Each selected geological parameter has a specific hydraulic sensitivity curve to erodibility (i.e., specific slope), where the slope is controlled mostly by P_a. However, plotting the calculated slopes of selected parameters versus selected P_a (i.e., 2, 10, and 40 kW/m^2) provides an overview of the relative importance of each parameter. This forms Step 7 (Figure 9) and is detailed in the Results section.

4 Results and discussion

4.1 Determining the hydraulic sensitivity curves to erodibility

The hydraulic sensitivity curves to erodibility for the selected parameters K_d, V_b, E_{doa}, *NPES*, and E_{rm} are shown in Figures 13a, 13b, 13c, 13d, and 13e, respectively. The classes of the analyzed geological parameters are represented by

average values. From Figure 13a, we note an inversely proportional relationship between K_d and erosion level; when K_d increases, the erosion level decreases. In Figure 13b, we adopt the rock block volume classification of Palmstrom (1995). As already observed for K_d, there is an inversely proportional relationship between V_b and erosion level; as V_b increases, erosion becomes less important. We adopt the E_{doa} classes in Figure 13c from Pells's classification (Pells 2016). Again, there is an inversely proportional relationship between E_{doa} and erosion level. There is a proportional relationship between *NPES* and erosion level (Figure 13d), as an increase in *NPES* produces a greater erosion level. Finally, we note an inversely proportional relationship between E_{rm} and erosion level, so that as E_{rm} decreases, erosion level increases (Figure 13e).

4.2 Determining the relative importance of the selected parameters

To determine the relative importance of the selected parameters (J_o, K_d, V_b, E_{doa}, *NPES*, and E_{rm}), we undertake the following steps:

1) For each geological parameter, we apply the three hydraulic sensitivity curves to erodibility (P_a = 2, 10, and 40 kW/m^2) to determine the slope value of each hydraulic sensitivity curve (the calculated slopes are presented in Table 9). The slope values are presented at a decimal precision to provide a more representative illustration of the behavior of rock as a function of hydraulic stream power. However, such an approach is solely adapted for analytical reasons and should not be used for design purposes;
2) For each geological parameter, the calculated slope values, corresponding to a P_a of 2, 10, and 40 kW/m^2, are plotted as a function of these P_a values (the produced curve is named hereafter as the slope variation curve);
3) All selected geological parameters are plotted and presented together (Figure 14).

Considering the calculated slopes of hydraulic sensitivity curves to erodibility (Table 9 and Figure 14), the selected parameters (for P_a = 2 kW/m^2) are ranked based on the slope of the hydraulic sensitivity curve from K_d (40.63°), *NPES* (29.43°), V_b (10.34°), J_o (6.49°), E_{doa} (3.41°), to E_{rm} (1.95°). The same pattern is observed for P_a = 10 and 40 kW/m^2. As slope results from the highest recorded erosion levels, K_d likely has a much greater role in hydraulic erosion than the other selected

parameters, as based on the used P_a values (2, 10, and 40 kW/m^2). In terms of relative importance in hydraulic erodibility, the selected parameters are ranked in importance (highest to lowest) from K_d, *NPES*, V_b, J_o, E_{doa}, and then E_{rm}. On the other hand, each selected parameter presents a distinct slope variation curve (i.e., the line connecting the calculated slopes of each parameter; Figure 14). Consequently, each parameter has a specific slope difference within the considered P_a interval (i.e., 2-40 kW/m^2). For example, the K_d slope difference is 7.73°, corresponding to a difference between the slope of 40 kW/m^2 (48.36°) and 2 kW/m^2 (40.63°). The selected parameters can therefore be ranked in terms of slope variation rate from highest to lowest as *NPES* (9.17), K_d (7.73), V_b (3.62), J_o (2.06), E_{doa} (1.72), and E_{rm} (0.60). This observation raises an important question as to what occurs when P_a is very high (e.g., 16 000 kW/m^2; Laugier et al., 2015). In these extreme cases, *NPES* may have a greater impact, given its steeper slope variation rate. If we extend the slope variation curves to these very (fictional) high P_a values (e.g., 100,000 kW/m^2), we observe that P_a is intense, the selected geological parameters maintain the same sequence, and maintain their relative importance in assessing the hydraulic erodibility of rock.

4.3 Comparisons with field observations

The *eGSI* index does not incorporate details related to joint opening; however, this approach is valid only when *GSI* is determined from the *GSI* reference (look-up) chart (Pells 2016) because this chart does not consider joint openings. On the other hand, when *GSI* is determined from *RMR*, here the joint opening is considered within factor F4 of the *RMR* system. Nonetheless, Pells (2016) recommended using the reference chart rather than the *RMR* system. The classification order of our geological parameters may only be compared with *RMEI* because the latter was proposed on the basis of field observations and takes into consideration joint openings as well as other geological parameters. However, it It is difficult to directly compare the *RMEI* classification system, developed based on field observation (Pells 2016), with our study results for three main reasons:

1) Some analyzed parameters, such as V_b, K_d, and E_{rm}, are not included as such in the *RMEI* system;

2) The analyzed parameters are evaluated separately in our study, while in the *RMEI* system, some geological parameters are presented together as one factor; for example, the nature of joint factors include joint roughness, joint aperture, and joint strength;

3) The relative importance of parameters in the *RMEI* classification system involves three levels (1 to 3), while our analysis identifies only two.

In our study, the first-level parameters include the K_d and *NPES* that, given their steep slopes, are deemed as the most important parameters controlling hydraulic erosion (Figure 15). The second-level parameters include V_b, J_o and E_{doa} that are relatively less important than the first-level parameters (Figure 15). *NPES* is identified as one of the most important parameters, both from our method and the field observations of Pells (2016). Rock block

shape, observed in the field as being relatively less important (*RF* = 1 in the *RMEI* classification system), is also determined through our analysis (as part of the E_{doa} parameter) to be less important than the first-level parameters (Figure 15). In the *RMEI* classification system (Pells 2016), the rock block size is not included directly. However, joint spacing (included as a factor in the *RMEI* classification system) provides an idea of rock block size, given that a greater spacing of joints begets a larger rock block volume than does a tight spacing of joints. Accordingly, the joint spacing factor of the *RMEI* classification system can be compared with the V_b parameter analyzed by our method. We also determine that the joint spacing factor (V_b parameter), considered in *RMEI* classification as a less important factor (*RF* = 1), falls into the second level of parameters (Figure 15). The J_o parameter is classified in the *RMEI* system as a second-level factor (*RF* = 2). In our analysis, we also find this parameter to be less important than the parameters of the first-level group. However, the J_o parameter in the *RMEI* classification system is included in the nature of the joint factor that combines joint opening and other joint conditions (i.e., joint roughness and strength). Joint roughness and strength can be considered as being synonymous with joint shear strength (K_d), which in our study is among the most important parameters. Combining the joint conditions highlights the importance of joint opening in the *RMEI* classification system. On the other hand, combining joint conditions downplays the importance of the joint roughness and strength (synonymous with K_d) that we determine as being very important parameters. This may explain the resultant committed error when the *RMEI* system is used to evaluate hydraulic rock scour (Section 2) despite *RMEI* being more sophisticated as it is based on field observations of eroded spillways. It should be noted that we could not compare the E_{rm} parameter as *RMEI* does not include this parameter or even a synonymous parameter.

5 Conclusion

We presented a comparative analysis of the existing methods for evaluating hydraulic rock scour, and this examination determined that existing methods are subjected to a given amount of error. As hydraulic conditions have less effect on the committed error, we focused particularly on geological parameters and determined the relative importance of the geological parameters that govern hydraulic erosion. We determined the relevance of the rock mass deformation module (E_{rm}) for evaluating the hydraulic rock scour and added E_{rm} to an existing set of relevant geological parameters. We then presented a methodology for identifying the relative importance of individual geological parameters within the set. For this, we assessed a suite of relevant parameters (K_d, J_o, *NPES*, V_b, E_{doa}, and E_{rm}) and found that the parameters could be classified in terms of their relative importance to hydraulic erodibility, from most to least important, as K_d, *NPES*, V_b, J_o, E_{doa}, then E_{rm}. This classification order generally agrees with classifications based on field observations.

Conflict of interest

The authors confirm that there are no known conflicts of interest associated with this publication and that no financial support for this work has influenced its outcome.

Acknowledgments

The authors would like to thank the organizations that have funded this project: Natural Sciences and Engineering Research Council of Canada (Grant No 498020-16), Hydro-Québec (NC-525700), and the Mitacs Accelerate program (Grant Ref. IT10008).

References

Annandale, G.W. 1995. Erodibility. *Journal of Hydraulic Research*, **33**, 471–494.

Annandale, G.W. 2006. *Scour Technology, Mechanics and Engineering in Practice*.

Annandale, G.W. and Kirsten, H.A.D. 1994. On the erodibility of rock and other earth materials. *Hydraulic Engineering*, **1**, 68–72.

Barton, N., Lien, R. and Lunde, J. 1974. Engineering classification of rock masses for the design of tunnel support. *Rock Mechanics*, **6**, 189–236.

Bieniawski, Z.T. 1973. Engineering Classification of Jointed Rock Masses. *The Civil Engineer in South Africa*, **15**, 343–353.

Bieniawski, Z.T. 1976. Rock mass classification in rock engineering. In Exploration for rock engineering, procedures of the symposium. *Z.T. Bieniawski, Cape Town: Balkema*, 97–106.

Bieniawski, Z.T. 1989. Engineering rock mass classifications : a complete manual for engineers and geologists in mining, civil, and petroleum engineering. 251.

Bollaert, E. and Schleiss, A. 2003. Scour of rock due to the impact of plunging high velocity jets Part I: A state-of-the-art review. *Journal of Hydraulic Research*, **41**, 451–464.

Boumaiza, L., Saeidi, A. and Quirion, M. 2019a. A method to determine the relevant geomechanical parameters for evaluating the hydraulic erodibility of rock. *Journal of Rock Mechanics and Geotechnical Engineering.*, **11**, 1004–1018.

Boumaiza, L., Saeidi, A. and Quirion, M. 2019b. Determining relative block structure rating for rock erodibility evaluation in the case of non-orthogonal joint sets. *Journal of Rock Mechanics and Geotechnical Engineering*, **11**, 72–87.

Castillo, L.G. and Carrillo, J.M. 2016. Scour, velocities and pressures evaluations produced by spillway and outlets of dam. *Water*, **8**, 1–21.

Cecil, O.S. 1970. *Correlations of Rock Bolt-Shotcrete Support and Rock Quality Parameters in Scandinavian Tunnels*.

Dooge, N. 1993. *Die Hidrouliese Erodeerbaarheid van Rotmassas in Onbelynde Oorlope Met Spesiale Verwysing Na Die Rol van Naatvulmateriaal*.

Douglas, K., Pells, S., Fell, R. and Peirson, W. 2018. The influence of geological conditions on erosion of unlined spillways in rock. *Quarterly Journal of Engineering Geology and Hydrogeology*, **51**, 219–228.

Fattahi, H., Varmazyari, Z. and Babanouri, N. 2019. Feasibility of Monte Carlo simulation for predicting deformation modulus of rock mass. *Tunnelling and underground space technology*, **89**, 151–156.

Hahn, W.F. and Drain, M.A. 2010. Investigation of the erosion potential of kingsley dam emergency spillway. *In*: *Proceeding of the Joint Annual Meeting and Conference of AIPG, AGWT, and the Florida Section of AIPG, Orlando, Florida, USA*. 1–10.

Henderson, F.M. 1966. *Open Channel Flow*.

Hoek, E. and Diederichs, M.S. 2006. Empirical estimation of rock mass modulus. *International Journal of Rock Mechanics and Mining Sciences*, **43**, 203–215.

Hoek, E., Kaiser, P.K. and Bawden, W.F. 1995. *Support of Underground Excavations in Hard Rock*.

Hoek, E., Corkum, B., Carranza-torres, C. and Corkum, B. 2002. Hoek-Brown failure criterion – 2002 Edition. *In*: *The Fifth North American Rock Mechanics Symposium, Toronto, Canada*. 267–273.

Jennings, J.E.., Brink, A.B.A. and Williams, A.A.B. 1973. Revised guide to soil profiling for civil engineering purposes in South Africa. *Civil Engineering in South Africa*, **15**, 3–12.

Kirsten, H.A.D. 1982. A classification system for excavation in natural materials. *The Civil Engineer in South Africa*, **24**, 292–308.

Kirsten, H.A.D. 1988. Case histories of groundmass characterization for excavatability. *Rock Classification Systems for Enginering Purposes. American Society for Testing and Materials, STP 984*, 102–120.

Kirsten, H.A.D., Moore, J.S., Kirsten, L.H. and Temple, D.M. 1996. Erodibility criterion for auxiliary spillways of dams. *In*: *ASAE International Meeting, Phoenix, Arizona, No. 962099*.

Kirsten, H.A.D., Moore, J.S., Kirsten, L.H. and Temple, D.M. 2000. Erodibility criterion for auxiliary spillways of dams. *International Journal of Sediment Research*, **15**, 93–107.

Laugier, F., Leturcq, T. and Blancer, B. 2015. Stabilité des barrages en crue : Méthodes d'estimation du risque d'érodabilité aval des fondations soumises à déversement par-dessus la crête. *In*: *Proceeding de La Fondation Des Barrages. Chambery, France*. 125–136.

Moore, J.S. 1991. *The Characterization of Rock for Hydraulic Erodibility*.

Moore, J.S., Temple, D.M. and Kirsten, H.A.D. 1994. Headcut advance threshold in earth

spillways. *Bulletin of the Association of Engineering Geologists*, **31**, 277–280.

Mörén, L. and Sjöberg, J. 2007. Rock erosion in spillway channels – A case study of the Ligga spillway. *In*: *Proceedings of 11th Congress of the International Society for Rock Mechanics, Lisbon, Portugal*. 87–90.

Mustafa, S., Khan, M.A., Khan, M.R., Hameed, F., Mughal, M.S., Asghar, A. and Niaz, A. 2015. Geotechnical study of marble, schist, and granite as dimension stone: a case study from parts of Lesser Himalaya, Neelum Valley Area, Azad Kashmir, Pakistan. *Bulletin of Engineering Geology and the Environment*, **74**, 1475–1487.

Mustafa, S., Khan, M.A., Khan, M.R., Sousa, L.M.O., Hameed, F., Mughal, M.S. and Niaz, A. 2016. Building stone evaluation-A case study of the sub-Himalayas, Muzaffarabad region, Azad Kashmir, Pakistan. *Engineering Geology*, **209**, 56–69.

Palmstrom, A. 1995. *RMi--a Rock Mass Characterization System for Rock Engineering Purposes*. Ph.D. thesis, University of Oslo, Norway.

Pells, S.E. 2016. *Erosion of Rock in Spillways*.

Pells, S.E., Pells, P.J.N., Peirson, W.L., Douglas, K. and Fell, R. 2015. Erosion of unlined spillways In Rock - does a 'scour threshold' exist? *In*: *Proceeding of Australian National Committee on Large Dams . Brisbane, Queensland, Australie*. 1–9.

Pitsiou, S. 1990. *The Effect of Discontinuites of the Erodibility of Rock in Unlined Spillways of Dams*.

Rock, A.J. 2015. *A Semi-Empirical Assessment of Plung Pool Scour: Two-Dimensional Application of Annandale's Erodibility Method on Four Dams in British Colombia, Canada*.

Rocsciences. 2019. https:/www.rocscience.com/.

Van-Schalkwyk, A. 1989. *Watenavorsingskommissie: Verslag Oor Loodsondersoek: Die Erodeebaarheid van Verskillende Rotsformasies in Onbeklede Damoorlope,*.

Van-Schalkwyk, A., Jordaan, J.M. and Dooge, N. 1994a. *Die Erodeerbaarheid van Verskillende Rotsformasies Onder Varierende Vloeitoestande*.

Van-Schalkwyk, A., Jordaan, J.M. and Dooge, N. 1994b. Erosion of rock in unlined spillways. *In*: *Proceeding of International Commission on Large Dams, Paris, 71 (37)*. 555–571.

Appendix 1. Summary of the data used in this study. Data are obtained from Pells (2016), except for that of MR, $E_{i,}$ and E_m.

ID	*GSI*	Rock type	*UCS* (MPa)	*MR*	E_i (GPa)	E_{rm} (GPa)	*N*	*eGSI*	*RMEI*	P_a (kW/m^2)	Observed scour
Ant. 1	55	Conglomerate	35.00	350	12.25	1.81	868	47	1188	1.7	Minor
Ant. 2	55	Conglomerate	35.00	350	12.25	1.81	575	47	243	0.8	Negligible
Ant. 3	55	Conglomerate	35.00	350	12.25	1.81	868	47	1440	0.7	Minor
Ant. 4	60	Conglomerate	35.00	350	12.25	2.46	1903	42	1080	6.3	Moderate
App.1	50	Sandstone	50.00	275	13.75	1.48	206	45	648	2.6	Negligible
App.2	50	Sandstone	50.00	275	13.75	1.48	206	43	648	15	Minor
Bro.1	70	Granite	100.00	425	42.50	14.35	3721	67	1440	6.4	Minor
Bro.2	70	Granite	100.00	425	42.50	14.35	2756	67	1296	28	Moderate
Bro.3	70	Granite	100.00	425	42.50	14.35	2233	55	1152	42	Moderate
Bro.4	70	Granite	100.00	425	42.50	14.35	2233	53	1080	56	Moderate
Bro.5	75	Granite	100.00	425	42.50	17.45	5629	65	432	28	Negligible
Bro.6	80	Granite	100.00	425	42.50	20.28	7003	77	144	37	Minor
Bro.7	70	Granite	100.00	425	42.50	14.35	2425	55	1440	56	Large
Bur.1	85	Ignimbrite	280.00	400	112.00	59.67	11417	82	252	165	Negligible
Bur.2	85	Ignimbrite	280.00	400	112.00	59.67	7848	80	288	165	Negligible
Bur.3	70	Ignimbrite	280.00	400	112.00	37.81	6089	60	972	165	Moderate
Bur.4	50	Ignimbrite	280.00	400	112.00	12.02	3653	40	1890	165	Large
Cat.1	85	Dolerite	140.00	350	49.00	26.11	3706	72	567	60	Minor
Cat.2	85	Dolerite	140.00	350	49.00	26.11	3706	72	126	60	Negligible
Cat.3	85	Dolerite	140.00	350	49.00	26.11	3706	72	567	60	Large
Cop.1	50	Granite	280.00	425	119.00	12.77	724	35	1620	5.7	Moderate
Cop.10	50	Granite	280.00	425	119.00	12.77	3721	25	1755	650	Extensive
Cop.11	50	Granite	280.00	425	119.00	12.77	724	35	1620	10	Minor
Cop.12	80	Granite	280.00	425	119.00	56.79	8372	70	1350	97	Moderate
Cop.13	80	Granite	280.00	425	119.00	56.79	8372	65	1350	145	Moderate
Cop.2	80	Granite	280.00	425	119.00	56.79	8372	70	1350	4.7	Minor
Cop.3	80	Granite	280.00	425	119.00	56.79	8372	65	1350	14	Moderate
Cop.4	50	Granite	280.00	425	119.00	12.77	3721	32	1755	34.7	Large
Cop.5	50	Granite	280.00	425	119.00	12.77	3721	32	1755	76.1	Extensive
Cop.6	50	Granite	280.00	425	119.00	12.77	3721	25	1755	47.1	Extensive
Cop.7	50	Granite	280.00	425	119.00	12.77	3721	32	1755	66.1	Moderate
Cop.8	75	Granite	280.00	425	119.00	48.86	7906	67	1485	95	Moderate
Cop.9	50	Granite	280.00	425	119.00	12.77	3721	32	1755	168	Large
Dar.1	65	Gneiss	140.00	525	73.50	19.51	4515	52	504	18	Minor
Dar.2	65	Gneiss	140.00	525	73.50	19.51	4515	52	1080	18	Moderate
Dar.3	65	Gneiss	140.00	525	73.50	19.51	4515	52	972	18	Moderate
Dar.5	65	Gneiss	140.00	525	73.50	19.51	4535	60	648	9	Minor
Dar.6	75	Gneiss	140.00	525	73.50	30.18	4651	-	2700	3.5	Large
Flo.1	68	Tillite	200.00	375	75.00	23.12	5495	43	-	120	Moderate
Flo.2	38	Tillite	100.00	375	37.50	1.96	100	13	-	120	Moderate
Gar.1	30	Schist	12.61	675	8.51	0.31	106	25	405	1	Negligible
Gar.2	30	Schist	12.61	675	8.51	0.31	106	23	-	14	Minor
Gar.4	30	Schist	12.61	675	8.51	0.31	106	25	405	1.3	Negligible
Gar.5	30	Schist	12.61	675	8.51	0.31	106	23	-	20	Minor
Goe.1	76	Tillite	140.00	375	52.50	22.29	2934	69	-	90	Minor
Goe.2	38	Tillite	35.00	375	13.13	0.68	26	31	-	90	Moderate
Goe.3	76	Tillite	140.00	375	52.50	22.29	2934	69	-	50	Negligible
Goe.4	38	Tillite	35.00	375	13.13	0.68	26	31	-	90	Moderate
Goe.5	38	Tillite	35.00	375	13.13	0.68	26	31	-	22	Moderate
Haa.1	20	Sandstone	12.61	275	3.47	0.09	11	5	3240	3.6	Large
Haa.2	55	Conglomerate	35.00	350	12.25	1.81	11	5	-	0.3	Moderate

ID	*GSI*	Rock type	*UCS* (MPa)	*MR*	E_i (GPa)	E_{rm} (GPa)	*N*	*eGSI*	*RMEI*	P_a (kW/m^2)	Observed scour
Haa.3	55	Conglomerate	35.00	350	12.25	1.81	11	5	3240	3.9	Large
Haa.4	20	Sandstone	12.61	275	3.47	0.09	11	5	-	2	Large
Har.1	20	Sandstone	12.61	275	3.47	0.09	1757	60	1296	0.6	Minor
Har.2	20	Sandstone	12.61	275	3.47	0.09	2283	65	1296	1	Minor
Har.3	65	Dolerite	140.00	350	49.00	13.00	4269	60	504	1	Minor
Har.4	70	Dolerite	140.00	350	49.00	16.54	5024	70	1980	56	Minor
Hart.1	65	Dolerite	140.00	350	49.00	13.00	3772	75	-	44	Negligible
Hart.2	80	Dolerite	140.00	350	49.00	23.38	36	31	-	50	Moderate
Hart.3	80	Quartzite	180.00	375	67.50	32.21	3772	75	-	18	Negligible
Kam.1	46	Quartzite	15.76	375	5.91	0.49	369	67	1008	4.5	Minor
Kam.2	80	Quartzite	180.00	375	67.50	32.21	6024	73	252	27	Negligible
Kam.3	74	Sandstone	140.00	275	38.50	15.26	61	31	1800	27	Moderate
Kam.4	80	Sandstone	140.00	275	38.50	18.37	61	13	-	49	Large
Kam.5	38	Sandstone	30.00	275	8.25	0.43	81	32	1080	14	Minor
Kli.1	38	Sandstone	30.00	275	8.25	0.43	11002	75	864	1.2	Negligible
Kli.2	37	Sandstone	30.00	275	8.25	0.41	6.1	23	1728	6	Minor
Kli.3	80	Dolerite	200.00	350	70.00	33.41	6.1	23	1728	11.4	Moderate
Kli.4	35	Dolerite	10.51	350	3.68	0.16	11002	73	864	6.5	Minor
Kli.5	35	Dolerite	10.51	350	3.68	0.16	6.1	23	1728	6.5	Minor
Kun.1	80	Dolerite	200.00	350	70.00	33.41	6038	67	594	35	Minor
Mac.1	35	Dolerite	10.51	350	3.68	0.16	128	27	1053	1.1	Minor

Mac.2	75	Quartzite	140.00	375	52.50	21.55	15	7	378	1.1	Minor
Mac.3	40	Greywacke	17.70	350	6.20	0.36	61	27	378	2.6	Minor
Mok.1	20	Greywacke	8.81	350	3.09	0.08	5385	67	630	0.6	Negligible
Mok.2	40	Greywacke	8.81	350	3.09	0.18	29	19	2025	1.4	Moderate
Mok.4	74	Sandstone	140.00	275	38.50	15.26	5385	67	630	1.3	Negligible
Mok.5	35	Sandstone	70.00	275	19.25	0.86	5385	67	630	3	Negligible
Mok.6	74	Sandstone	140.00	275	38.50	15.26	29	19	2025	20	Large
Mok.8	74	Sandstone	140.00	275	38.50	15.26	5385	67	630	2.3	Negligible
Mok.9	35	Sandstone	70.00	275	19.25	0.86	29	19	2025	180	Extensive
Moo.1	74	Sandstone	140.00	275	38.50	15.26	110	51	594	0.3	Minor
Moo.2	35	Sandstone	70.00	275	19.25	0.86	110	51	594	0.2	Negligible
Moo.3	60	Sandstone	17.70	275	4.87	0.98	110	42	2925	27	Moderate
Moo.4	60	Sandstone	17.70	275	4.87	0.98	110	42	2925	17	Minor
Osp.1	60	Sandstone	17.70	275	4.87	0.98	1053	46	972	1.6	Negligible
Osp.2	60	Sandstone	17.70	275	4.87	0.98	108	25	1404	13.2	Moderate
Osp.3	58	Sandstone	40.00	275	11.00	1.96	1053	46	972	1.9	Minor
Osp.4	45	Sandstone	30.00	275	8.25	0.65	108	33	1404	13.2	Moderate
Osp.5	58	Sandstone	40.00	275	11.00	1.96	1053	41	972	2.2	Negligible
Pin.1	45	Sandstone	30.00	275	8.25	0.65	310	45	1440	4.8	Minor
Pin.2	58	Sandstone	40.00	275	11.00	1.96	157	31	1440	4.8	Moderate
Pin.3	55	Rhyolitic	70.00	400	28.00	4.13	558	45	2160	0.4	Moderate
Pin.4	45	Rhyolitic	70.00	400	28.00	2.19	523	32	2520	28	Large
Row.1	55	Rhyolitic	70.00	400	28.00	4.13	4883	65	162	13	Negligible
Row.2	50	Rhyolitic	70.00	400	28.00	3.00	7104	44	936	13	Moderate
Spl.1	75	Quartzite	280.00	375	105.00	43.11	2664	72	864	120	Moderate
Spl.2	65	Quartzite	280.00	375	105.00	27.87	4729	77	864	120	Negligible
Spl.3	75	Greywacke	140.00	350	49.00	20.12	359	57	1080	24	Minor
Way.1	80	Greywacke	140.00	350	49.00	23.38	6089	67	1080	8.6	Negligible
Way.2	60	Greywacke	80.00	350	28.00	5.62	4871	67	1404	8.6	Negligible
Way.3	80	Dolerite	140.00	350	49.00	23.38	1282	57	1728	8.6	Moderate
Way.4	80	Dolerite	140.00	350	49.00	23.38	44	2	-	22	Moderate

Appendix 2. Sensitivity curves to erodibility based on (a) K_d, (b) V_b, (c) E_{doa}, (d) *NPES* classifications (Boumaiza et al., 2019b).

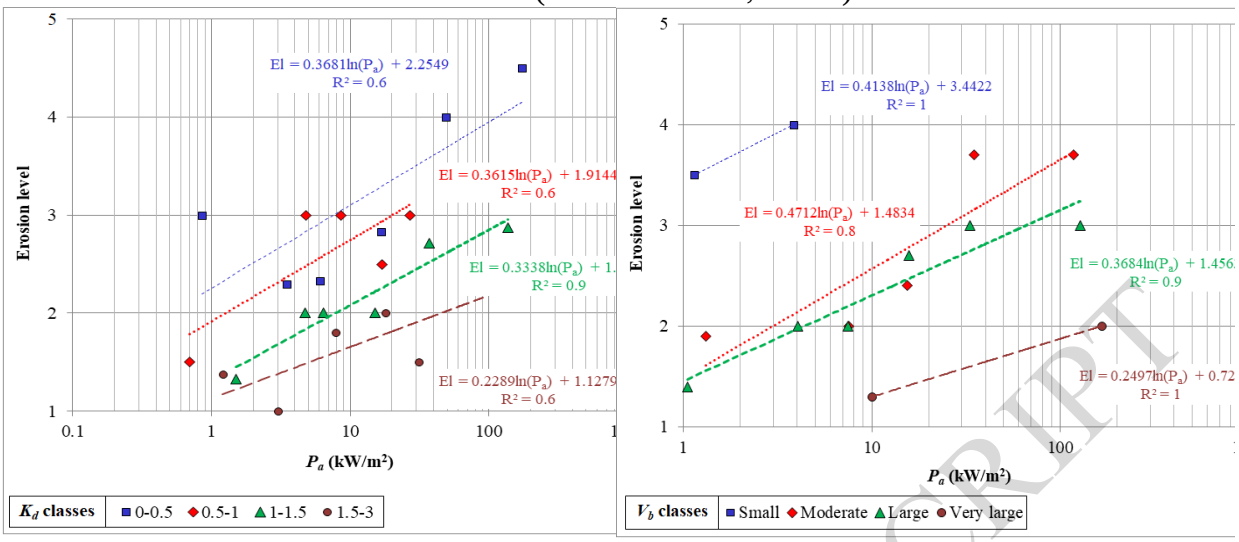

(a)

(b)

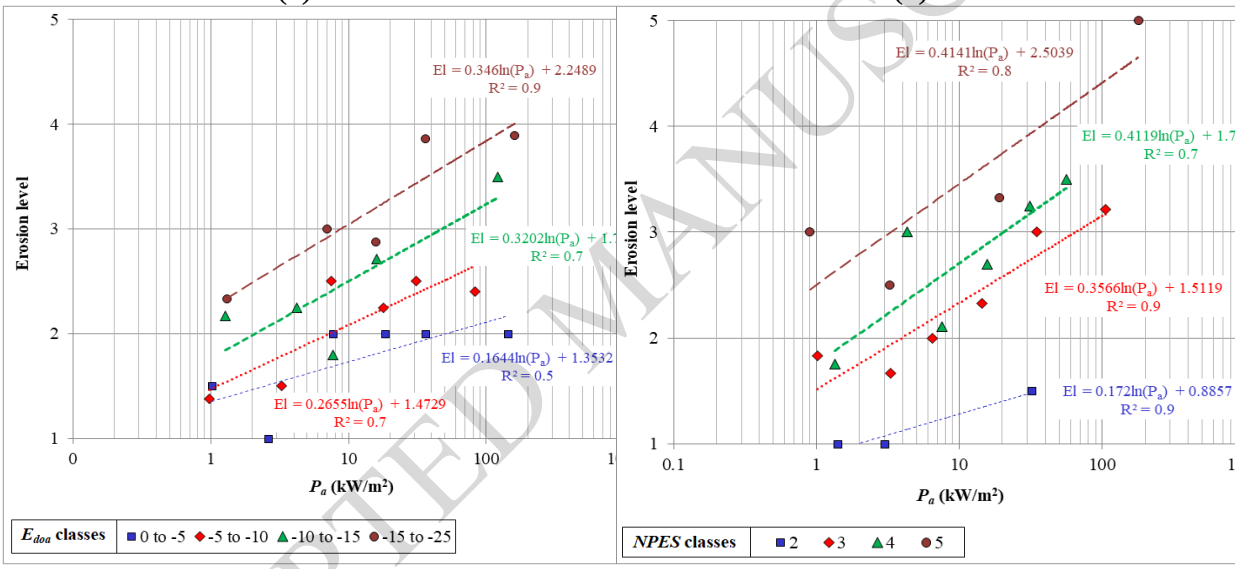

(c)

(d)

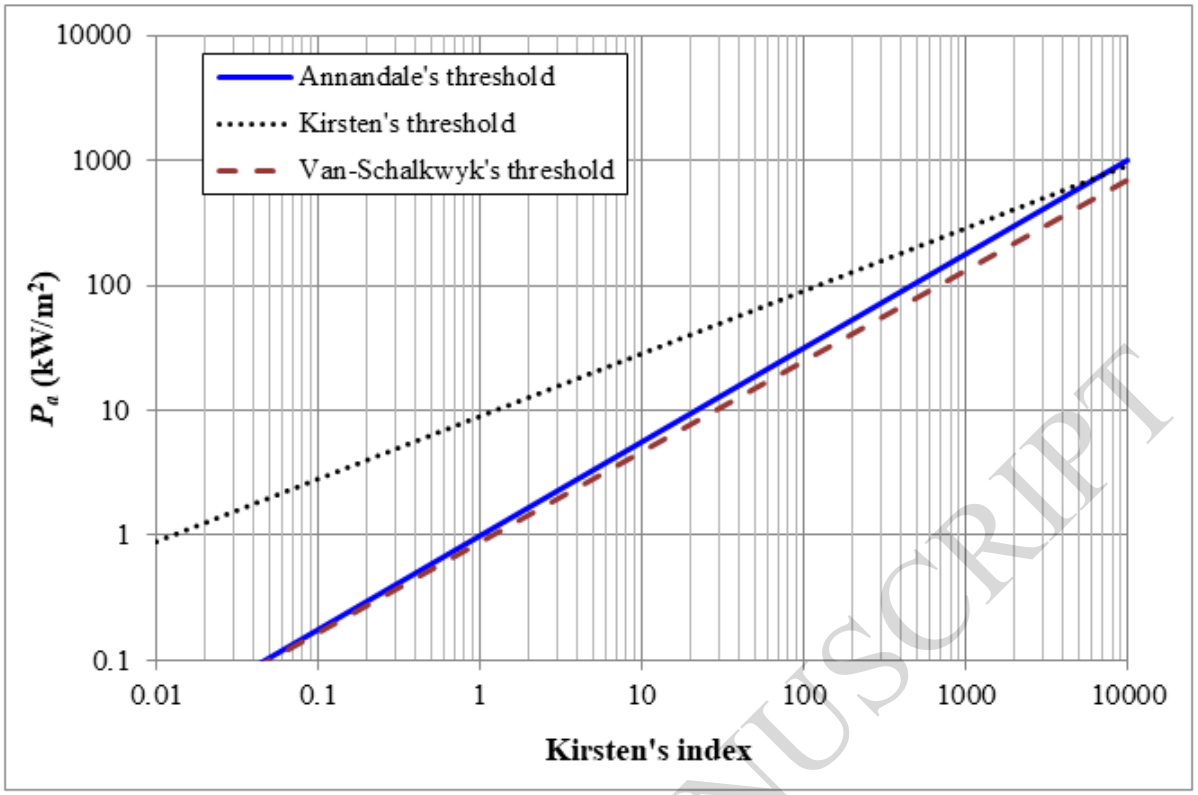

Figure 1. Comparison of scour threshold lines.

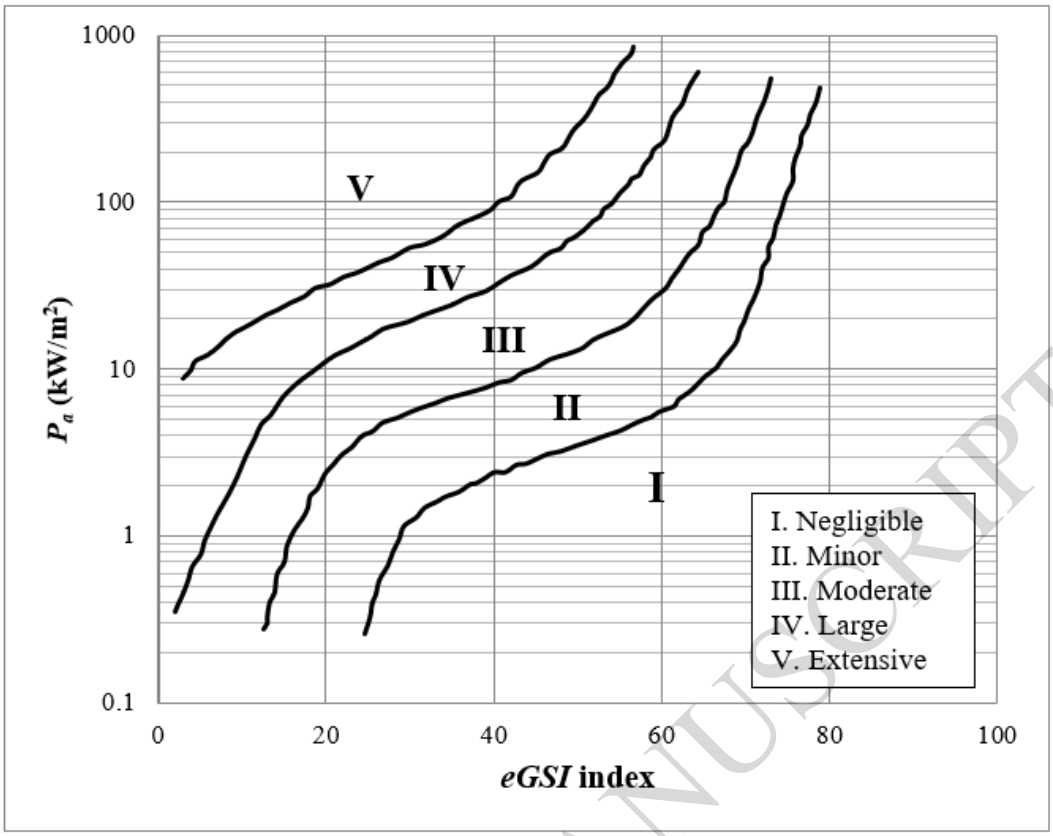

Figure 2. Erosion classes as determined based on the *eGSI* index (reproduced from Pells, 2016).

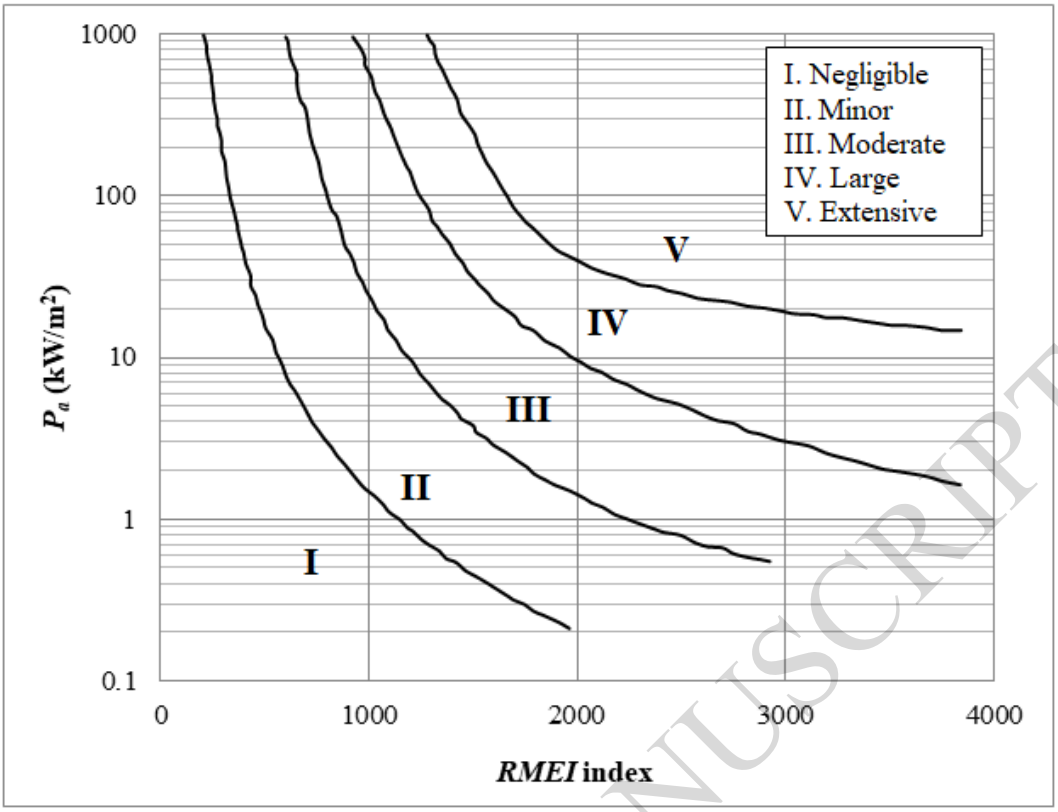

Figure 3. Erosion classes as determined based on the *RMEI* index (Douglas *et al.* 2018).

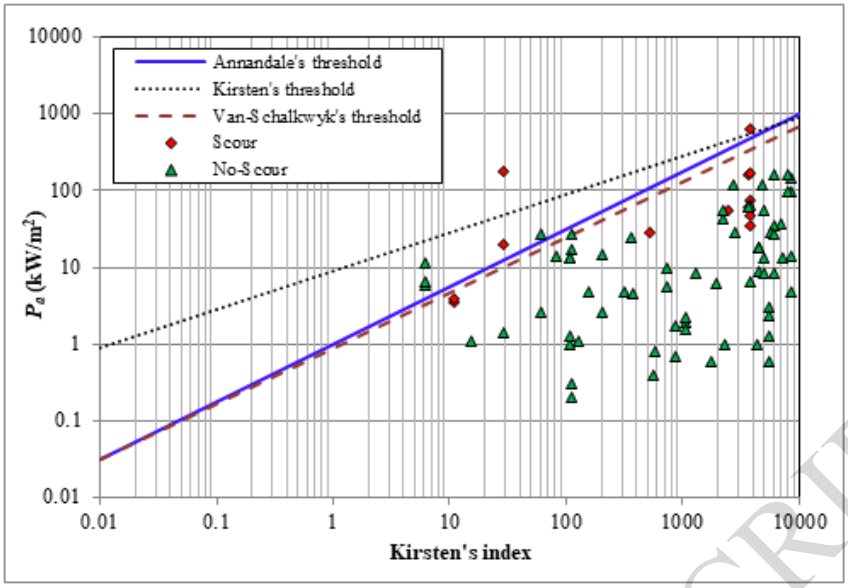

(a)

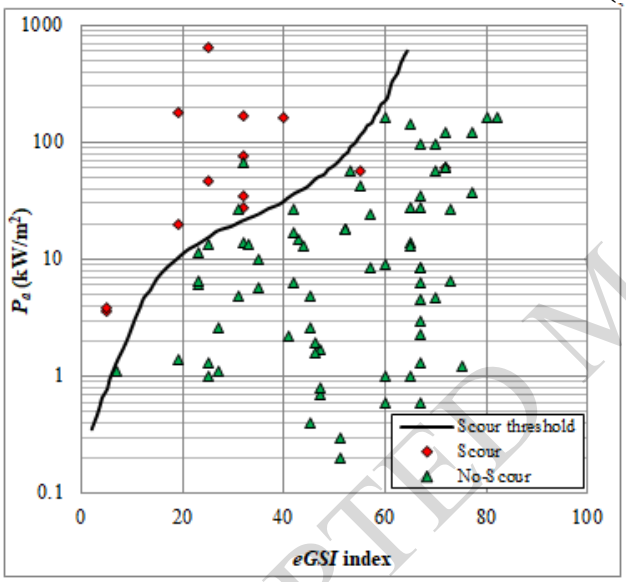

(b)

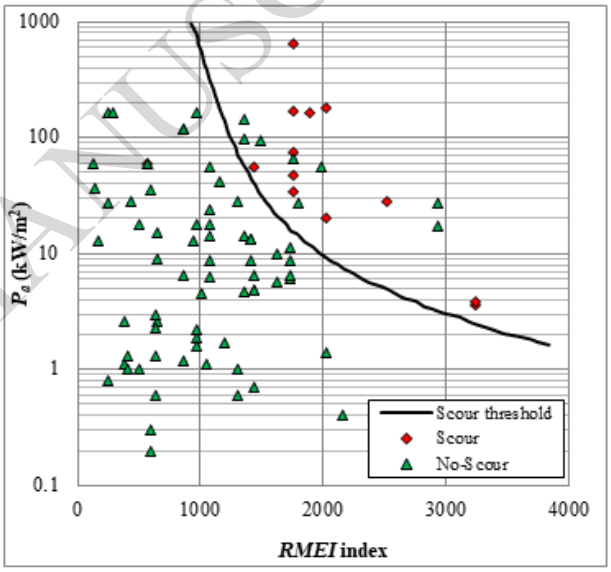

(c)

Figure 4. Plots of the 86 case studies according to (a) Kirsten's index, (b) the *eGSI* index, and (c) the *RMEI* index.

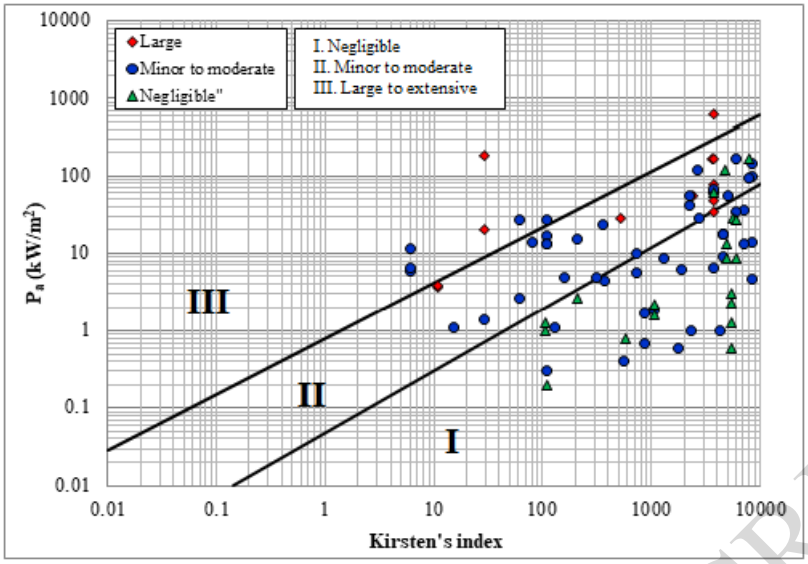

(a)

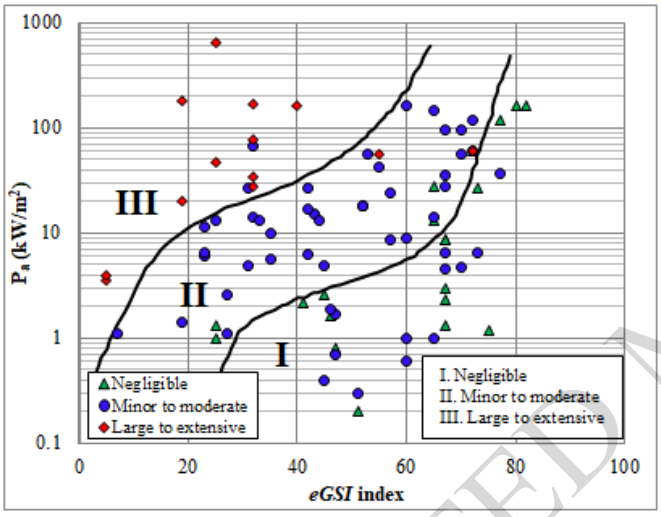

(b)

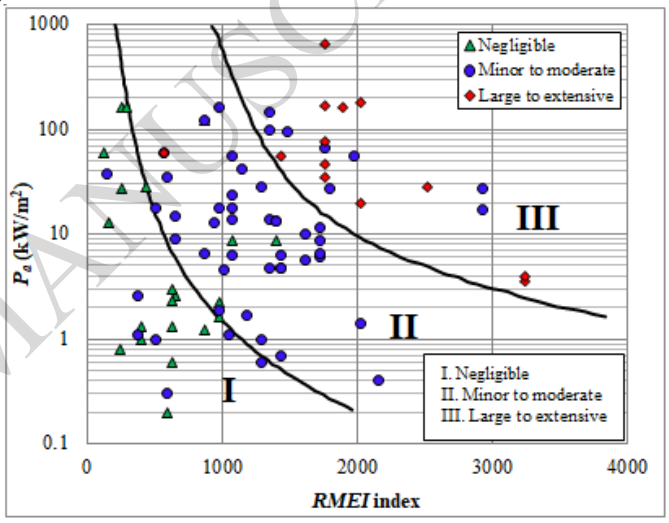

(c)

Figure 5. Plotted data based on (a) Kirsten's index, (b) *eGSI* index, (c) *RMEI* index by considering three erosion classes.

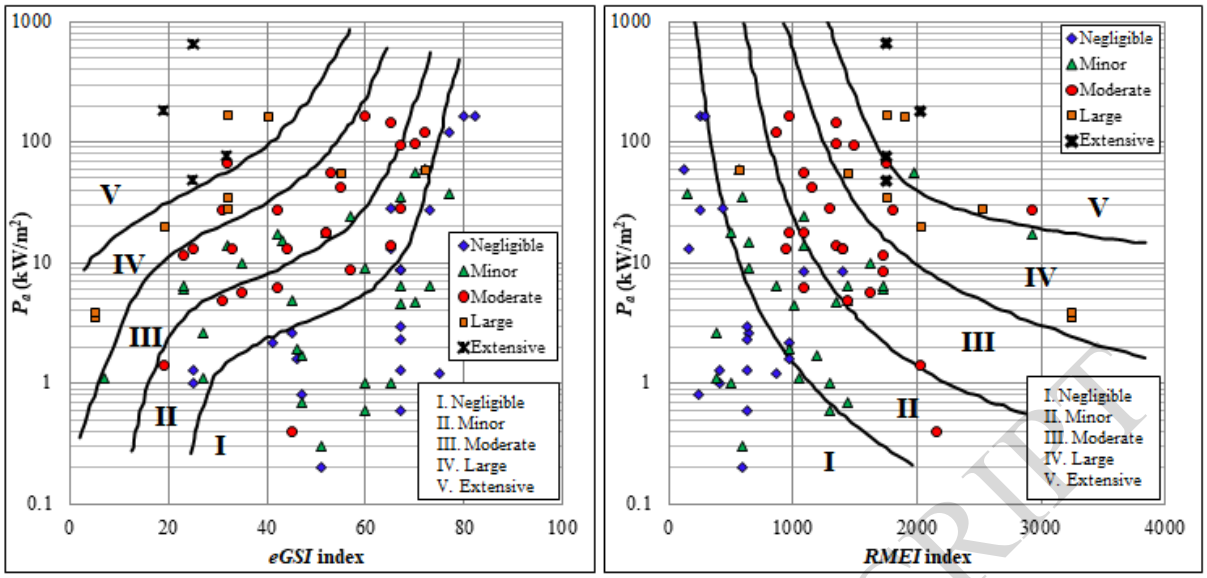

(a) (b)

Figure 6. Plotted data based on the (a) *eGSI* index and (b) *RMEI* index with five erosion classes

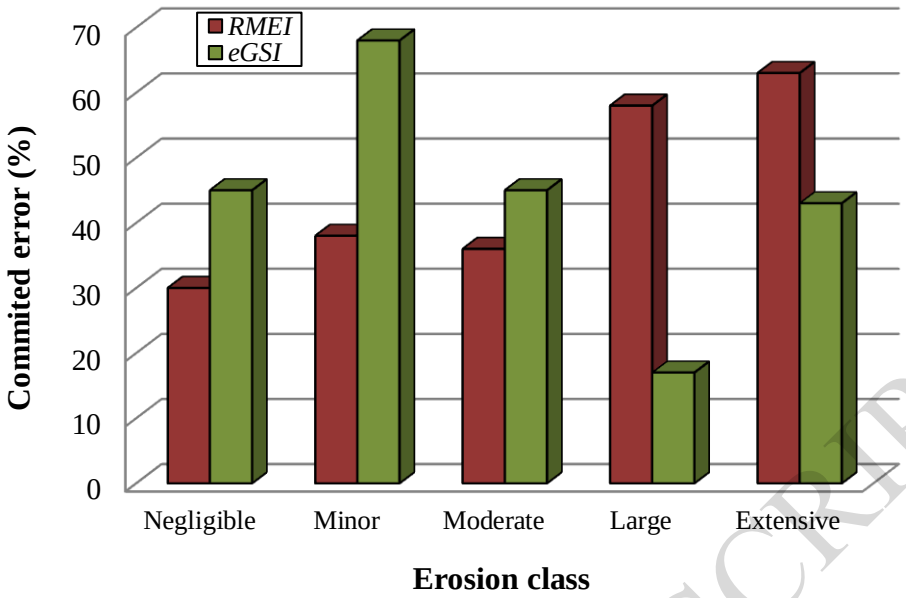

Figure 7. Committed errors within the different erosion classes.

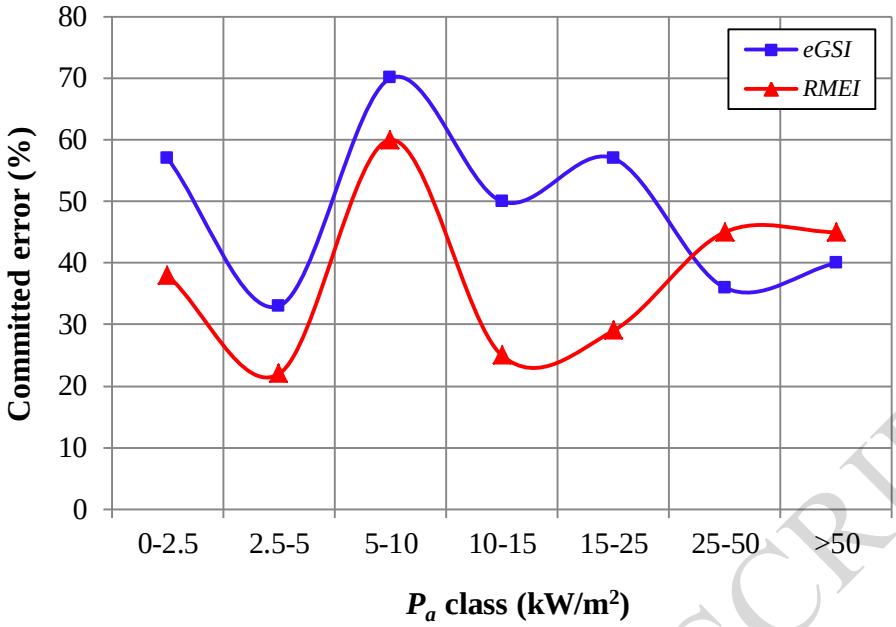

Figure 8. Committed errors for the various P_a classes.

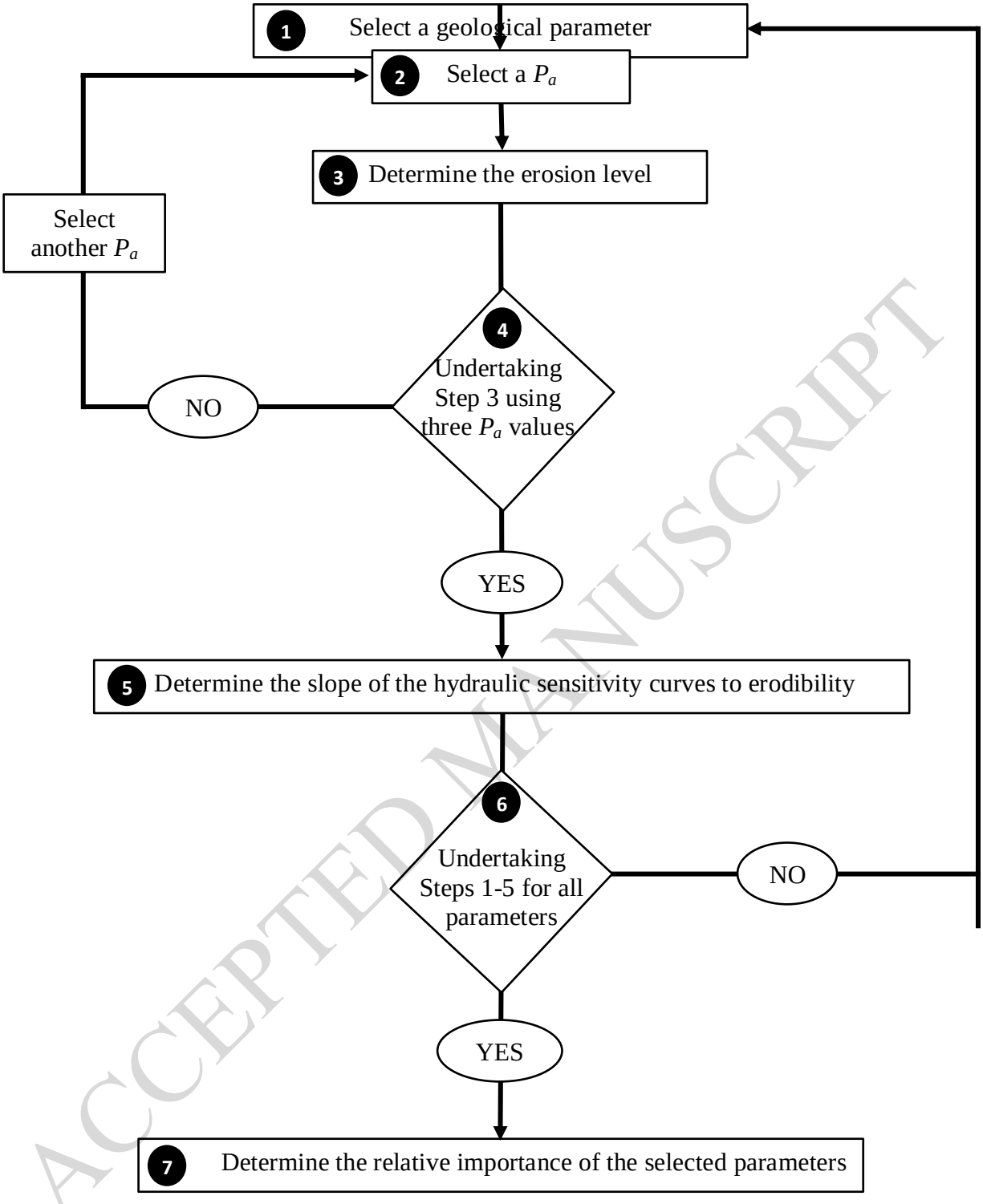

Figure 9. Algorithm for determining the relative importance of selected parameters. The confirmations YES and NO are presented as a reminder to confirm that the preceding step has been completed (YES) or remains to be completed (NO).

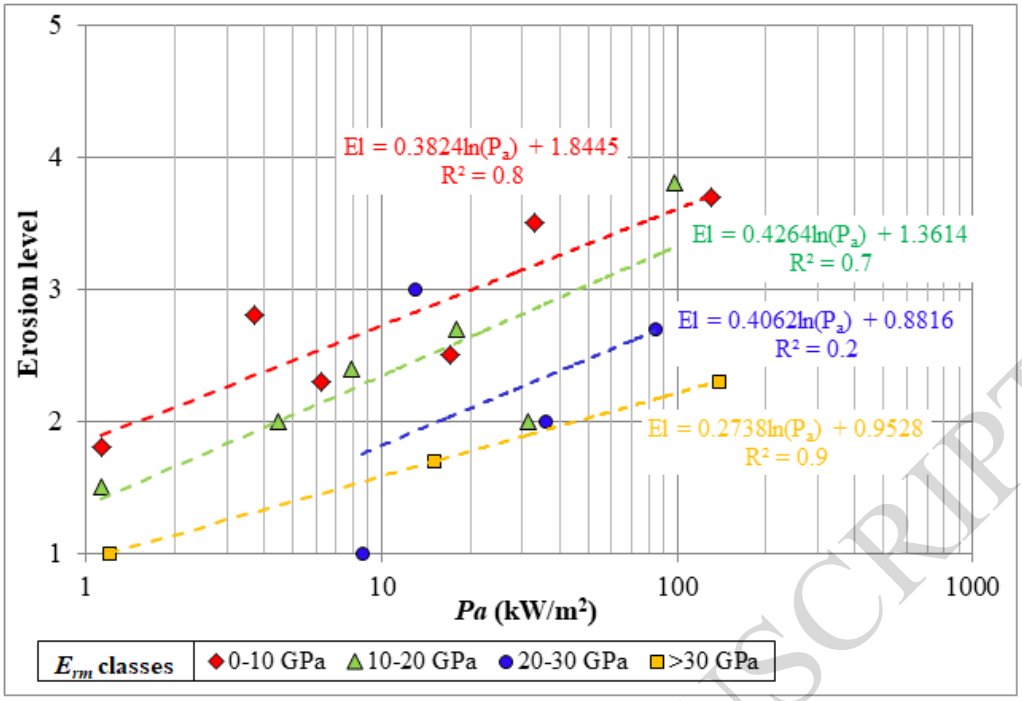

Figure 10. Sensitivity curves to erodibility based on E_{rm} classification. Each best-fit line corresponds to symbol data points of the same color and shape (e.g., the best-fit blue line corresponds to the blue circles), and the associated equation is also of the same color.

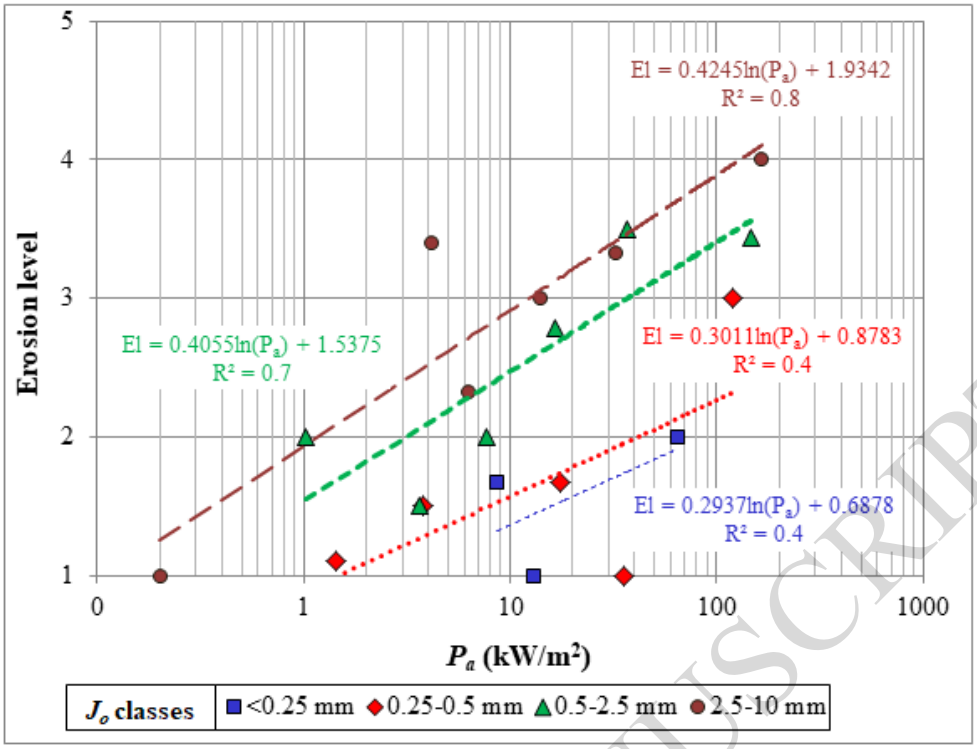

Figure 11. Sensitivity curves to erodibility based on J_o classification (Boumaiza *et al.* 2019a).

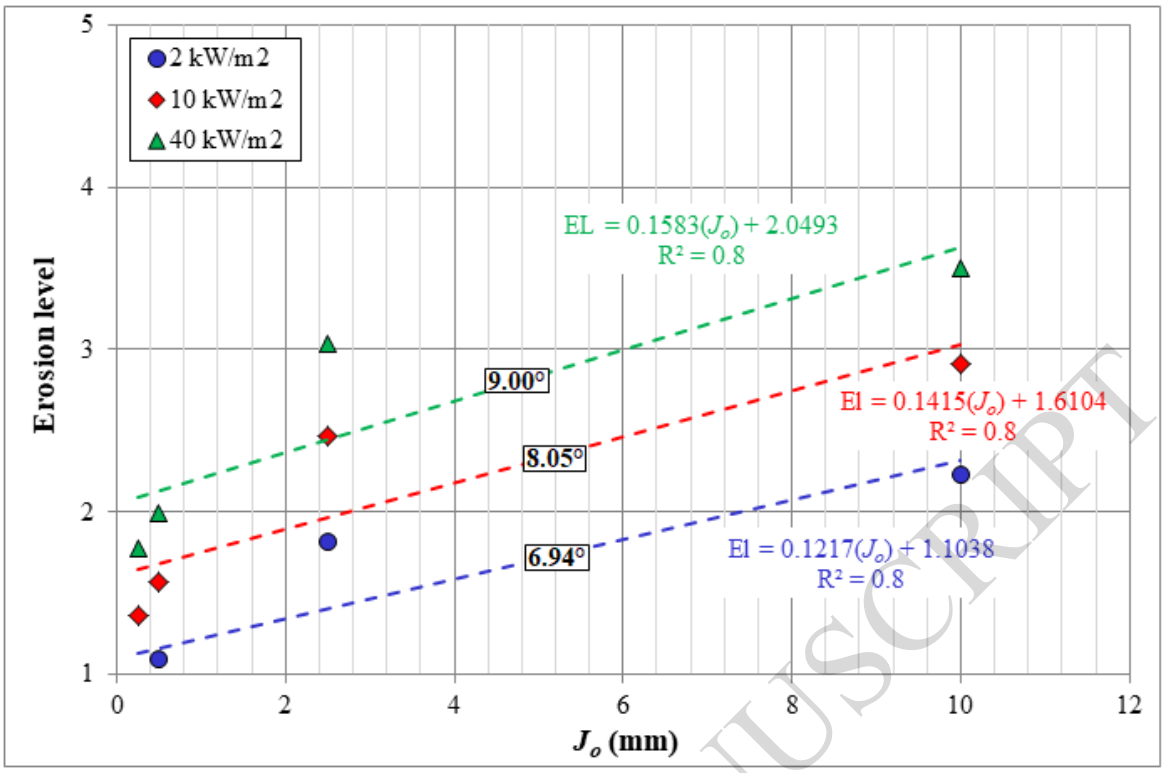

Figure 12. J_o hydraulic sensitivity curves to erodibility.

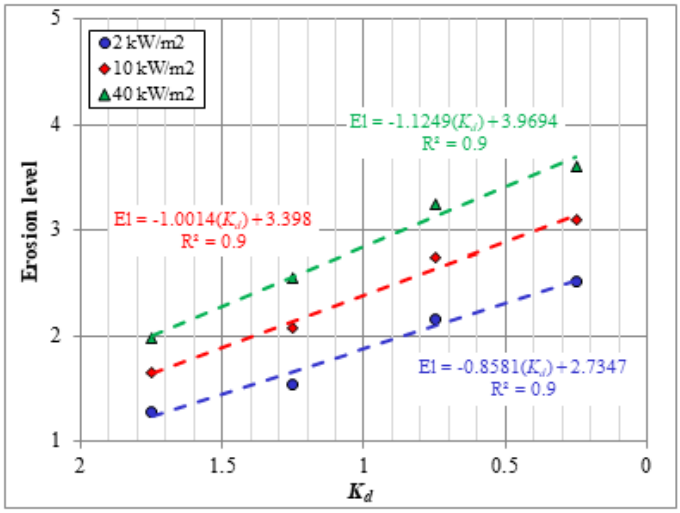

(a)

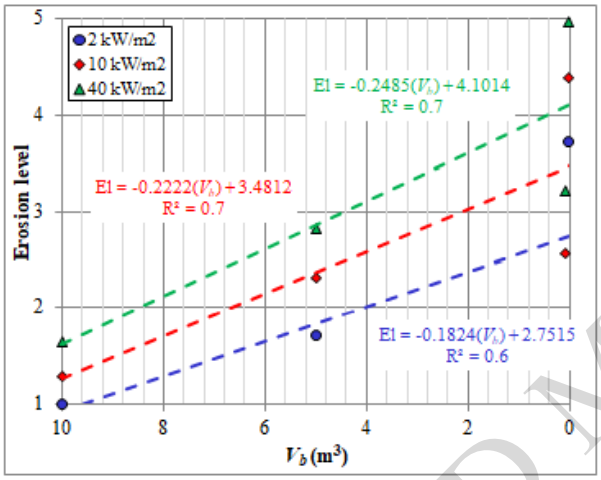

(b)

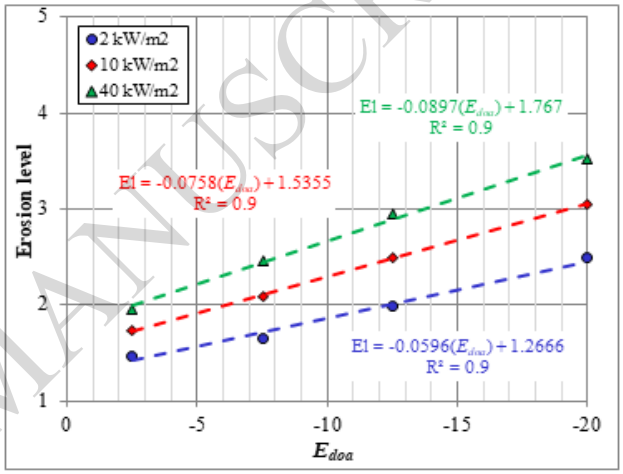

(c)

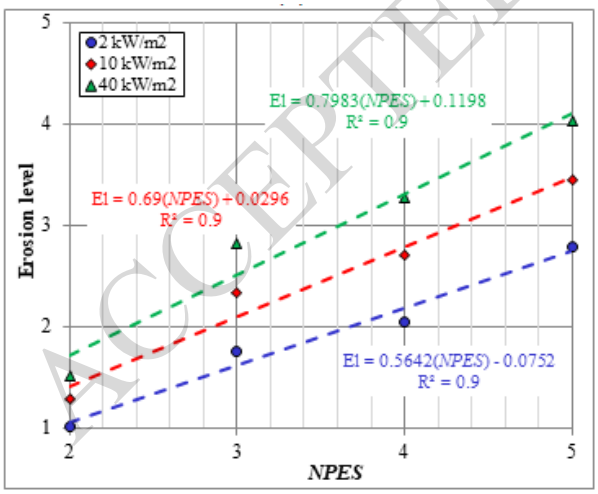

(d)

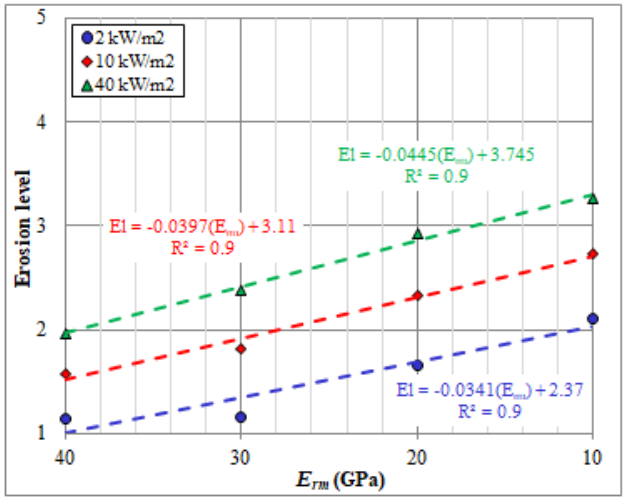

(e)

Figure 13. Hydraulic sensitivity curves for (a) K_d, (b) V_b, (c) E_{doa}, (d) *NPES*, and (e) E_{rm}. Note that for the hydraulic sensitivity curves of K_d, V_b, E_{doa}, and E_{rm}, the x-axis values are presented from higher to lower values.

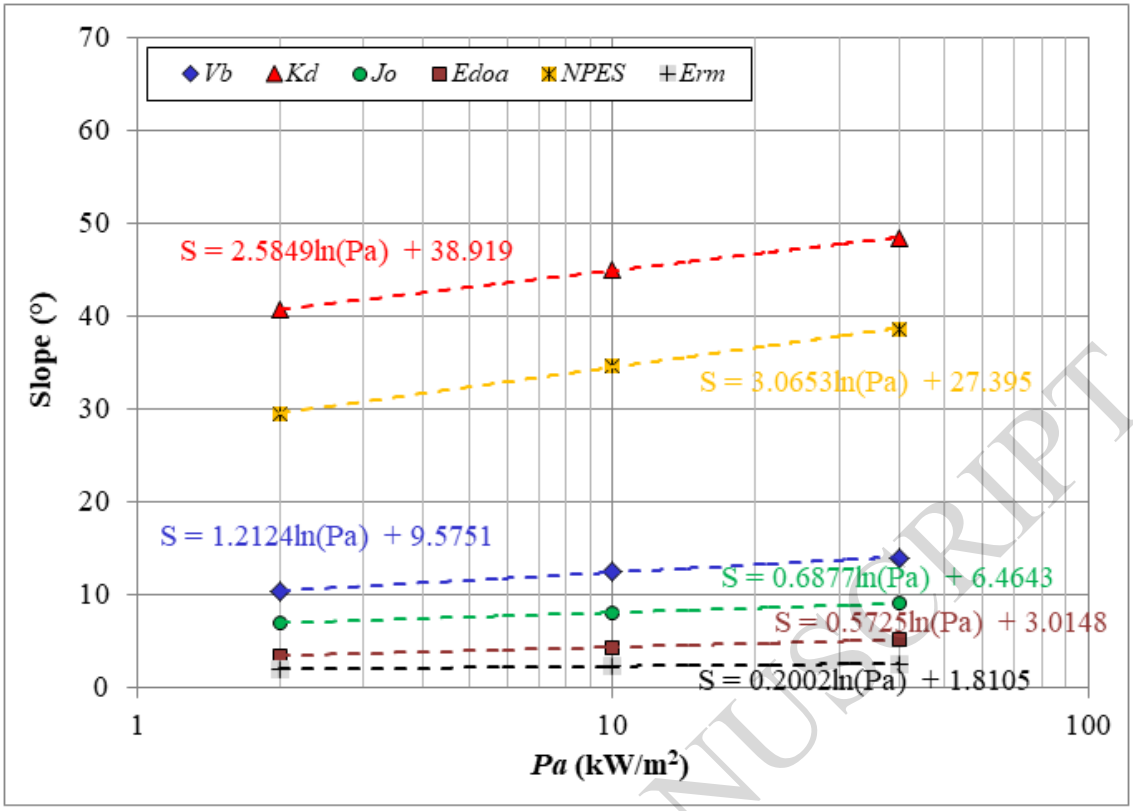

Figure 14. Slope variation curves of the selected parameters.

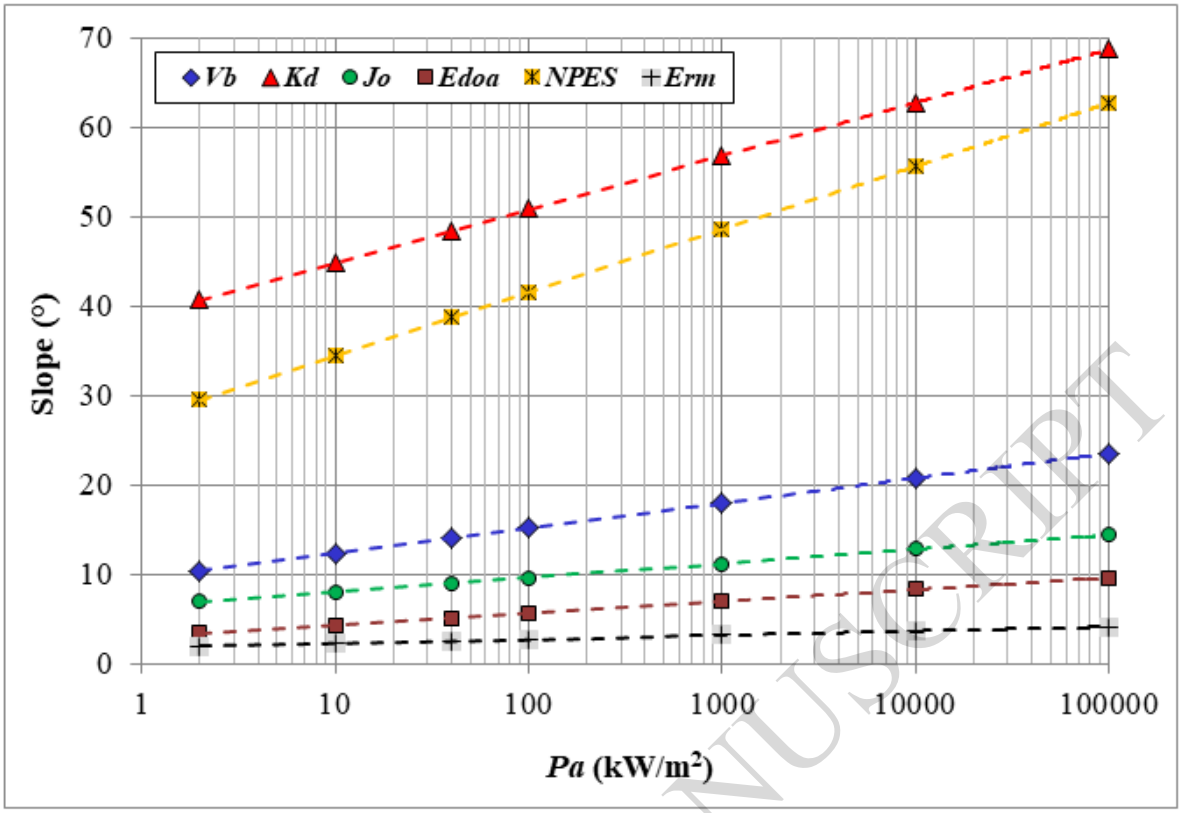

Figure 15. Extended slope variation curves of the selected parameters.

Table 1. Classification of the erosion (Van Schalkwyk et al., 1994a).

Depth of erosion (m)	Erosion class
0	None
0–1	Little
1–5	Moderate
>5	Extensive

Table 2. Classification of the erosion (Van Schalkwyk et al., 1994b).

Depth of erosion (m)	Erosion class
<0.2	Negligible
0.2–0.5	Minor
0.5–2	Moderate
>2	Large

Table 3. Description of erosion conditions (Pells 2016).

Max. depth (m)	General extent (m^3/100 m^2)	Descriptor
<0.3	<10	Negligible
0.3–1	1–30	Minor
1–2	30–100	Moderate
2–7	100–350	Large
>7	>350	Extensive

Table 4. Committed error calculated based on the various methods.

Method	Number of poorly evaluated case studies	Committed error (%)
Annandale, Van Schalkwyk (same threshold)	14	16
Kirsten	11	13
eGSI	4	5
RMEI	9	10

Table 5. Committed error calculated according to the Van Schalkwyk and the Pells's methods (*eGSI* and *RMEI*).

	Van Schalkwyk	***eGSI***	***RMEI***
Erosion class	**Committed error (%)**		
Negligible	14	24	19
Minor to moderate	46	29	29
Large to extensive	77	15	8

Table 6. Committed error calculated from the *RMEI* and *eGSI* methods.

	eGSI	***RMEI***
Erosion class	**Committed error (%)**	
Negligible	45	30
Minor	68	38
Moderate	45	36
Large	17	58
Extensive	43	63

Table 7. The proposed E_{rm} classification.

Class	E_{rm} **(GPa)**	**Description**
1	0–10	Very low deformation modulus
2	10–20	Low deformation modulus
3	20–30	Moderate deformation modulus
4	>30	High deformation modulus

Table 8. Calculated erosion level based on J_o classification.

	J_o (mm)			
	<0.25 mm	**0.25–0.5 mm**	**0.5–2.5 mm**	**2.5–10 mm**
P_a (kW/m^2)	**Calculated erosion level**			
2 kW/m^2	0.89	1.09	1.82	2.23
10 kW/m^2	1.36	1.57	2.47	2.91
40 kW/m^2	1.77	1.99	3.03	3.50

Table 9. Determined slopes of hydraulic sensitivity curves to erodibility.

	Selected parameters					
	J_o	K_d	V_b	E_{doa}	*NPES*	E_{rm}
P_a (kW/m^2)	**Calculated slopes**					
2	6.94°	40.63°	10.34°	3.41°	29.43°	1.95°
10	8.05°	45.04°	12.53°	4.33°	34.46°	2.27°
40	9.00°	48.36°	13.96°	5.13°	38.60°	2.55°